

A Multistage Full in Phase P–stable Scheme with Optimized Properties

Xin Shi^a, Theodore E. Simos^{1b,c,d,e}

^a*School of Information Engineering, Chang'an University,
Xi'an, P. R. China, 710064*

^b*Department of Mathematics, College of Sciences, King Saud University,
P. O. Box 2455, Riyadh 11451, Saudi Arabia*

^c*Group of Modern Computational Methods,
Ural Federal University, 620002, 19 Mira Street,
Ekaterinburg, Russian Federation*

^d*Data Recovery Key Laboratory of Sichuan Province,
Neijiang Normal University, Dongtong Road 705,
Neijiang 641100, China*

^e*Section of Mathematics, Department of Civil Engineering,
Democritus University of Thrace,
Xanthi, Greece (Visiting Professor) tsimos.conf@gmail.com*

(Received June 3, 2019)

Abstract

A fourteen algebraic order P–stable symmetric four–stages two–step scheme with zeroing phase–lag and its derivatives up to order three, is constructed, for the first time in the literature, in this paper. The new four–stages method is built based on the following procedure:

- Gratification of the conditions for the characteristic of the P–stability (necessary and sufficient).
- Gratification of the condition of the zeroing of the phase–lag.
- Gratification of the junctures of the zeroing of the derivatives of the phase–lag up to order three.

¹Corresponding author. Highly Cited Researcher, Active Member of the European Academy of Sciences and Arts, Active Member of the European Academy of Sciences, Corresponding Member of European Academy of Arts, Sciences and Humanities

The above procedure leads to the construction, for the first time in the literature, of a four-stages P-stable fourteen algebraic order symmetric two-step method with phase-lag and its first, second and third derivatives equal to zero.

For the newly introduced method, a numerical and theoretical analysis is presented, which consists of the following stages:

- the construction of the newly introduced four-stages method,
- the feat of the determination of its local truncation error (LTE),
- the development of the asymptotic form of the LTE of the newly introduced four-stages method,
- the determination of the stability and interval of periodicity of the newly introduced four-stages method,
- the determination of an embedded algorithm and the definition of the variable step methodology for the foundation of the step sizes,
- the estimation of the computational effectiveness of the newly introduced four-stages method which consists of its application on:
 - the resonance problem of the radial Schrödinger equation and on
 - the system of the coupled differential equations arising from the Schrödinger equation.

Based on the above research, we conclude that the newly introduced four-stages method is more efficient than the existed ones.

1 Introduction

In the presented paper we develop, for the first time in the literature, a newly introduced scheme with zeroing phase-lag and its derivatives up to order three.

The development of the newly introduced scheme follows the below mentioned levels:

- Levelness 1: Contentment of the characteristic of the P-stability.
- Levelness 2: Contentment of the characteristic for the zeroing of the phase-lag.
- Levelness 3: Contentment of the characteristics for the zeroing of the derivatives of the phase-lag up to order three.

The test for the efficiency of the newly introduced algorithm will be based on:

- the radial time independent Schrödinger equation and
- Systems of coupled differential equations of the Schrödinger type.

The effective approximate solution of the above problems is very important in Computational Chemistry (see [10] and references therein) since the Schrödinger equation is an important part of the quantum chemical computations (see [10] and references therein). The numerical solution of the Schrödinger equation is needed in problems with more than one particle. The efficient approximate solution of the Schrödinger equation (using numerical methods) gives the following important information:

- computations of molecular properties (vibrational energy levels and wave functions of systems) and
- presentation of the electronic structure of the molecule (see for more details in [11–14]).

An embedded numerical scheme will be also developed. The scheme will be based on an local truncation error control technique and a variable–step procedure. This newly embedded scheme is based on the newly introduced method.

The problems which are investigated in this paper belong to the following category of special problems:

$$\varepsilon''(x) = f(x, \varepsilon), \quad \varepsilon(x_0) = \varepsilon_0 \quad \text{and} \quad \varepsilon'(x_0) = \varepsilon'_0. \quad (1)$$

which have periodical and/or oscillating solutions.

The main families of the numerical schemes and their literature is presented below:

1. Exponentially, trigonometrically and phase fitted Runge–Kutta and Runge–Kutta Nyström algorithms: [48], [51], [60], [63] – [68], [57] [79], [86] – [97]. This family of methods contains Runge–Kutta and Runge–Kutta Nyström schemes. This family is divided into two subcategories:

- Numerical methods with the property of accurate integration of sets of functions of the form:

$$\begin{aligned} x^i \cos(\omega x), \quad i = 0, 1, 2, \dots \quad \text{or} \quad x^i \sin(\omega x), \quad i = 0, 1, 2, \dots \\ \text{or} \quad x^i \exp(\omega x), \quad i = 0, 1, 2, \dots \end{aligned} \quad (2)$$

or sets of functions which are combination of the above functions.

- Numerical methods with the property of zeroing of the phase–lag and its derivatives.

Remark 1. *The frequency of the problem in (2) is denoted by the quantity ω .*

2. Multistep exponentially, trigonometrically and phase fitted methods and multistep schemes with minimal phase-lag: [1]– [8], [19]– [22], [26]– [29], [35], [39], [41], [45], [49]– [50], [54], [59], [61]– [62], [72]– [74], [80]– [83]. This family of schemes contains multistep algorithms. The family is divided into two subcategories:
 - Multistep methods with the property of accurate integration of sets of functions of the form (2) or sets of functions which are combination of the functions mentioned in (2).
 - Multistep methods with the property of zeroing of the phase-lag and its derivatives.
3. Symplectic integrators: [43]– [44], [52], [55], [58], [68]– [71], [77]. This family of methods contains schemes for which the Hamiltonian energy of the system remains almost constant during the integration procedure.
4. Nonlinear algorithms: [53]. This family of methods contains algorithms with nonlinear form (i.e. the relation between several approximations of the function on several points of the integration domain (i.e. y_{n+j} , $j = 0, 1, 2, \dots$) is nonlinear).
5. General algorithms: [15]– [18], [23]– [25], [36]– [38], [42]. This family of methods contains numerical algorithms with constant coefficients.

2 The construction of symmetric multistep algorithms

The theory for the construction of the symmetric $2m$ algorithms - where m is the number of steps - is the subject of the present section.

The usage of the the symmetric $2m$ algorithms, which are members of the family of the finite difference methods and which are defined by (4), means that the procedure for the solution of problems of the form (1) will be the discretization of the area of integration, which is symbolized as $[a, b]$.

We use the following symbols:

- h represents the step length of the integration \equiv with the stepsize of the discretization.

Definition 1.

$$h = |x_{i+1} - x_i|, \tag{3}$$

with the parameter i to be moved between $1 - m$ and $m - 1$ with step 1 ($i = 1 - m(1)m - 1$)

- x_k denotes the k -th point on the discretization domain.
- ε_k denotes the approximation of the function $\varepsilon(x)$ at the point x_k . The approximation ε_k is determined using 2 m -step method (4) presented below

A general form of the family of 2 m -step algorithms is given by:

$$\Delta(m) : \sum_{i=-m}^m \alpha_i \varepsilon_{n+i} = h^2 \sum_{i=-m}^m \beta_i f(x_{n+i}, \varepsilon_{n+i}) \tag{4}$$

where α_i and β_i $i = -m(1)m$ are the coefficients of the 2 m -step scheme.

Definition 2.

$$\Delta(m) \rightarrow \begin{cases} \beta_m \neq 0 & \text{implicit;} \\ \beta_m = 0 & \text{explicit.} \end{cases} \tag{5}$$

Definition 3.

$$\Delta(m) \text{ with } \alpha_{i-m} = \alpha_{m-i}, \beta_{i-m} = \beta_{m-i}, i = 0(1)m \rightarrow \text{symmetric} \tag{6}$$

Remark 2. The scheme $\Delta(m)$ is connected with the following linear operator

$$L(x) = \sum_{i=-m}^m \alpha_i \varepsilon(x + i h) - h^2 \sum_{i=-m}^m \beta_i \varepsilon''(x + i h) \tag{7}$$

where $\varepsilon \in \mathbb{C}^2$ (i.e. $\mathbb{C}^2 \equiv \mathbb{C} \times \mathbb{C}$).

Definition 4. [15] We call a multistep scheme (4) that is of an algebraic order v , if the linear operator L (7) is zeroed for any linear combination of the linearly independent functions $1, x, x^2, \dots, x^{v+1}$.

Application of the symmetric 2 m -step scheme $\Delta(m)$ into the model equation

$$\varepsilon'' = -\phi^2 \varepsilon \tag{8}$$

leads to the difference equation:

$$\begin{aligned} \Sigma_m^4(v) \varepsilon_{n+m} + \dots + \Sigma_1^4(v) \varepsilon_{n+1} + \Sigma_0^4(v) \varepsilon_n \\ + \Sigma_1^4(v) \varepsilon_{n-1} + \dots + \Sigma_m^4(v) \varepsilon_{n-m} = 0 \end{aligned} \quad (9)$$

and its connected characteristic equation:

$$\begin{aligned} \Sigma_m^4(v) \lambda^m + \dots + \Sigma_1^4(v) \lambda + \Sigma_0^4(v) \\ + \Sigma_1^4(v) \lambda^{-1} + \dots + \Sigma_m^4(v) \lambda^{-m} = 0. \end{aligned} \quad (10)$$

where

- $v = \phi h$,
- h is the step length or stepsize of the integration and
- $\Sigma_j^4(v)$, $j = 0(1)m$ are the stability polynomials.

Definition 5. [16] *A symmetric 2m-step scheme is called that has an non zero interval of periodicity $(0, v_0^2)$, if its characteristic equation (10) has the following roots :*

$$\lambda_1 = e^{i\psi(v)}, \lambda_2 = e^{-i\psi(v)}, \text{ and } |\lambda_i| \leq 1, i = 3(1)2m \quad (11)$$

for all $v \in (0, v_0^2)$, where $\psi(v)$ is a real function of v .

Definition 6. (see [16]) *A symmetric multistep method is called **P-stable** if its interval of periodicity is equal to $(0, \infty)$.*

Remark 3. *A symmetric multistep algorithm is called **P-stable** if the following necessary and sufficient conditions are hold:*

$$|\lambda_1| = |\lambda_2| = 1 \quad (12)$$

$$|\lambda_j| \leq 1, j = 3(1)2m, \forall v. \quad (13)$$

Definition 7. *A symmetric multistep algorithm is called **singularly P-stable** if its interval of periodicity is equal to $(0, \infty) \setminus T$, where T is a finite set of points.*

Definition 8. [17], [18] *A symmetric multistep algorithm with connected characteristic equation given by (10), has phase-lag which is defined by the leading term in the expansion of*

$$t = v - \psi(v). \tag{14}$$

If $t = O(v^{\gamma+1})$ as $v \rightarrow \infty$ then we say that the order of the phase-lag is equal to γ .

Definition 9. [19] *A symmetric multistep algorithm is called **phase-fitted** if its phase-lag is equal to zero.*

Theorem 1. [17] *For a symmetric 2m-step method, with characteristic equation given by (10), a direct formula for the determination of the phase-lag order Ω^4 and the phase-lag constant ν is given by*

$$-\nu v^{\Omega^4+2} + O(v^{\Omega^4+4}) = \frac{2 \Sigma_m^4(v) \cos(mv) + \dots + 2 \Sigma_j^4(v) \cos(jv) + \dots + \Sigma_0^4(v)}{2 m^2 \Sigma_m^4(v) + \dots + 2 j^2 \Sigma_j^4(v) + \dots + 2 \Sigma_1^4(v)} \tag{15}$$

The Theorem 1 leads us to the following conclusion:

Conclusion 1. *For the family of symmetric two-step methods the phase-lag order Ω^4 and the phase-lag constant ν can be determined directly using the formula:*

$$-\nu v^{\Omega^4+2} + O(v^{\Omega^4+4}) = \frac{2 \Sigma_1^4(v) \cos(v) + \Sigma_0^4(v)}{2 \Sigma_1^4(v)} \tag{16}$$

where $\Sigma_j^4(v) j = 0, 1$ are the stability polynomials.

3 A new four-stages P-stable symmetric method with expunged phase-lag and its first and second derivatives

Our research will focus to the following family of schemes:

$$\begin{aligned} \widehat{\varepsilon}_{n+1} &= \varepsilon_{n+1} - h^2 \left(c_1 f_{n+1} - c_0 f_n + c_1 f_{n-1} \right) \\ \widetilde{\varepsilon}_{n+1} &= \varepsilon_{n+1} - h^2 \left(c_3 \widehat{f}_{n+1} - c_2 f_n + c_3 f_{n-1} \right) \\ \check{\varepsilon}_{n+1} &= \varepsilon_{n+1} - h^2 \left(c_5 \widetilde{f}_{n+1} - c_4 f_n + c_5 f_{n-1} \right) \\ \varepsilon_{n+1} + a_1 \varepsilon_n + \varepsilon_{n-1} &= h^2 \left[b_1 \left(\check{f}_{n+1} + f_{n-1} \right) + b_0 f_n \right] \end{aligned} \tag{17}$$

where $f_{n+i} = \varepsilon''(x_{n+i}, \varepsilon_{n+i})$, $i = -1(1)1$, $\widehat{f}_{n+1} = \varepsilon''(x_{n+1}, \widehat{q}_{n+1})$, $\widetilde{f}_{n+1} = \varepsilon''(x_{n+1}, \widetilde{\varepsilon}_{n+1})$, $\check{f}_{n+1} = \varepsilon''(x_{n+1}, \check{\varepsilon}_{n+1})$ and $a_1, b_i, i = 0, 1$ and $c_j, j = 0(1)5$ are parameters.

Remark 4. We call the new scheme hybrid or nonlinear (since it has four stages) and all the approximations are based on the point x_{n+1} .

We study the following specific case:

$$\begin{aligned} b_0 &= \frac{5}{6}, b_1 = \frac{1}{12}, c_3 = \frac{2347}{173838}, \\ c_4 &= \frac{4139}{84370}, c_5 = \frac{4139}{168740}. \end{aligned} \tag{18}$$

If we apply the new algorithm (17) with the coefficients given by (18) to the scalar test equation (8), we obtain the difference equation (9) with $m = 1$ and the corresponding characteristic equation (10) with $m = 1$, where:

$$\begin{aligned} \Sigma_1^4(v) &= 1 + \frac{1}{12}v^2 + \frac{4139v^4}{2024880} + \frac{2347v^6}{85044960} + \frac{2347v^8c_1}{85044960} \\ \Sigma_0^4(v) &= a_1 + \frac{5}{6}v^2 - \frac{4139v^4}{1012440} - \frac{4139v^6c_2}{2024880} - \frac{2347v^8c_0}{85044960} \end{aligned} \tag{19}$$

In the flowchart of Figure 1 we present the platforms for the construction of the new scheme (for construction of flowcharts in LaTeX one can see [100]):

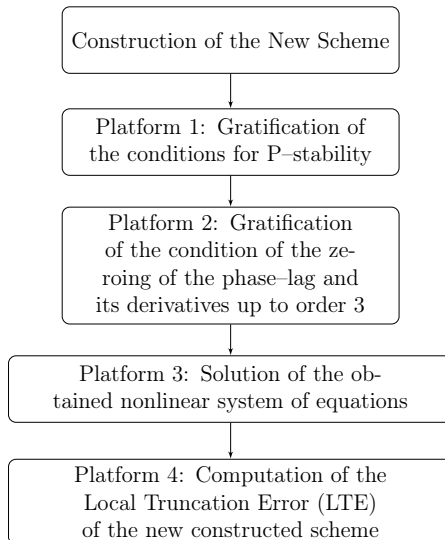


Figure 1. Development of the newly introduced symmetric algorithm

3.1 Gratification of the cuonditions for P–stability

In order to obtain the gratification of the conditions for the P–stability for the newly introduced algorithm, we use the methodology developed by Lambert and Watson [16] and Wang [84]:

- In order to gratify the characteristic equation given by (10) for $m = 1$ for $\lambda = e^{Iv}$, where $I = \sqrt{-1}$, we obtain the following equation:

$$(e^{Iv})^2 \Sigma_0^4(v) + e^{Iv} \Sigma_1^4(v) + \Sigma_0^4(v) = 0 \tag{20}$$

- In order to gratify the characteristic equation given by (10) for $m = 1$ for $\lambda = e^{-Iv}$, where $I = \sqrt{-1}$, we obtain the following equation:

$$(e^{-Iv})^2 \Sigma_0^4(v) + e^{-Iv} \Sigma_1^4(v) + \Sigma_0^4(v) = 0 \tag{21}$$

Remark 5. *The conditions for P–stability (20) and (21) are produced using:*

- *the Definition 5*
- *the characteristic equation given by (10) with $m = 1$, where Σ_j^4 , $j = 0, 1$ given by (19).*

3.2 Gratification of the condition of the zeroing of the phase–lag and its derivatives up to order 3

The gratification of the condition of the zeroing of the phase–lag and its derivatives up to order 3, for the newly introduced scheme (17) with coefficients give by (18), leads to the system of equations:

$$\text{Phase – Lag(PL)} = \frac{1}{2} \frac{\Upsilon_0}{\Upsilon_4} = 0 \tag{22}$$

$$\text{First Derivative of the Phase – Lag} = \frac{\Upsilon_1}{\Upsilon_4^2} = 0 \tag{23}$$

$$\text{Second Derivative of the Phase – Lag} = \frac{\Upsilon_2}{\Upsilon_4^3} = 0 \tag{24}$$

$$\text{Third Derivative of the Phase – Lag} = \frac{\Upsilon_3}{\Upsilon_4^4} = 0 \tag{25}$$

where $\Upsilon_j(v)$, $j = 0(1)4$ are given in the Appendix A.

3.3 Solution of the produced system of nonlinear equations determined by (20)–(25)

The solution of the nonlinear system of equations produced by (20), (21), (22)–(25), leads to the the coefficients of the newly introduced scheme:

$$\begin{aligned} a_1 &= \frac{\Upsilon_5}{\Upsilon_6} c_0 = \frac{\Upsilon_7}{9388 v^8 \Upsilon_8} \\ c_1 &= -\frac{\Upsilon_9}{2347 v^8 \Upsilon_8} c_2 = -\frac{\Upsilon_{10}}{521514 v^5 \Upsilon_8} \end{aligned} \quad (26)$$

where $\Upsilon_j(v)$, $j = 5(1)10$ are given in the Appendix B.

The probability, during the integration procedure, of impossibility of determination of the coefficients (26) - a reason, for example, can be that the denominators of (26) $\rightarrow 0$ for some values of $|v|$ - leads us to give the truncated Taylor series expansions of the coefficients developed in (26) in the Appendix C.

The behavior of new obtained coefficients is presented in Figure 1.

Since we have determined the coefficients of the newly introduced scheme, we can determine its local truncation error (*LTE*):

$$\begin{aligned} LTE_{NM4SPS3DV} &= -\frac{53}{161653459968000} h^{16} \left(5 \varepsilon_n^{(16)} + 80 \phi^6 \varepsilon_n^{(10)} \right. \\ &\quad \left. + 150 \phi^8 \varepsilon_n^{(8)} + 80 \phi^{10} \varepsilon_n^{(6)} \right. \\ &\quad \left. + 5 \phi^{16} \varepsilon_n \right) + O(h^{18}). \end{aligned} \quad (27)$$

The newly introduced method is symbolized as *NM4SPS3DV*, since it is a Four–Stages P–Stable Scheme with Vanished Phase–Lag and its Derivatives up to Order Three.

Remark 6. *Based on the LTE given by (27) we can*

- *define the algebraic order of the newly introduced scheme*
- *obtain the asymptotic form of the LTE for a specific problem, which will be used for the evaluation of the effectiveness of the newly introduced scheme.*

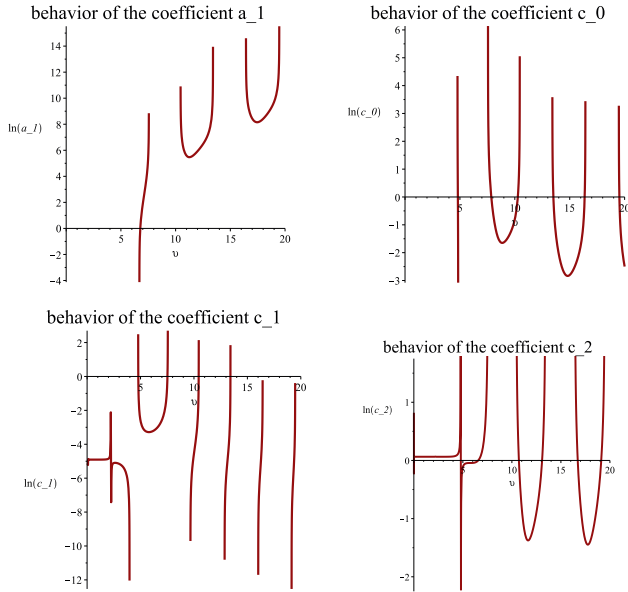


Figure 2. Behavior of the coefficients of the new four–stages method (17) given by (26) for several values of $v = \phi h$.

4 Error and stability analysis of the newly introduced algorithm

4.1 Comparative error analysis

The local truncation error of some four–stages schemes will be investigated in this section.

Our study will be based on the test model:

$$\varepsilon''(x) = (V(x) - V_c + \Gamma) \varepsilon(x) \quad (28)$$

where

- $V(x)$ determines the potential function,
- V_c determines a constant approximation of the potential on the specific point x ,

- $\Gamma = V_c - E$
- $\Xi(x) = V(x) - V_c$ and
- E denotes the energy.

Remark 7. *It is obvious from (28) that the test model is the radial time independent Schrödinger equation with potential $V(x)$.*

We will evaluate the following algorithms:

4.1.1 Classical method (i.e., method (17) with constant coefficients)

$$LTE_{CL} = -\frac{53}{32330691993600} h^{16} \varepsilon_n^{(16)} + O(h^{18}). \quad (29)$$

4.1.2 P-stable method with vanished phase-lag and its first and second derivatives developed in [9]

$$LTE_{NM4SPS2DV} = -\frac{53}{161653459968000} h^{16} \left(5 \varepsilon_n^{(16)} + 32 \phi^6 \varepsilon_n^{(10)} + 30 \phi^8 \varepsilon_n^{(8)} - 3 \phi^{16} \varepsilon_n \right) + O(h^{18}). \quad (30)$$

4.1.3 P-stable method with vanished phase-lag and its first, second and third derivatives developed in Section 3

The Local Truncation Error for this newly introduced scheme is given by (27)

For the comparative local truncation error analysis we use the following procedure:

- Layer 1: Application of the *LTE* formulae given by (29), (30) and (27) to the model problem (28).
- Layer 2: Using Layer 1, we obtain the new formulae of *LTE*.

Remark 8. *The technique used for the development of the new formulae of *LTE* consists of the following steps:*

1. *Production of the derivatives of the function ε up to order 16, which are symbolized like DER_j^i , $j = 1(1)16$, using the scalar model (28)). Some formulae of the derivatives of the function ε are given in the Appendix D.*

2. Substitution of DER_e^j , $j = 1(1)16$ in the formulae given by (29), (30) and (27).
3. Final development of the new formulae of LTE.

- Layer 3: Investigation of the new formulae of LTE \Rightarrow observation on the parameter Γ and the energy E .

The general form of the new formulae of LTE is given by:

$$LTE = h^p \sum_{j=0}^k \Phi_j \Gamma^j \quad (31)$$

with Φ_j :

1. real numbers (frequency independent cases i.e. the classical case) or
2. formulae of v and Γ (frequency dependent schemes),

p is the algebraic order of the scheme under evaluation and k is the maximum possible power of Γ in the formulae of LTE.

- Layer 4: We study two set of values for the parameter Γ :

1. The Energy is Closed to the Potential.

Resultants:

$$\Gamma \approx 0 \Rightarrow \Gamma^i \approx 0, \quad i = 1, 2, \dots \quad (32)$$

which leads to:

$$LTE_{\Gamma=0} = h^k \zeta_0 \quad (33)$$

Remark 9. The quantity ζ_0 is the same for all the schemes of the same family, i.e. $LTE_{CL} = LTE_{NM4SPS2DV} = LTE_{NM4SPS3DV} = h^{16} \zeta_0$. ζ_0 is given in the Appendix E.

Theorem 2. (32) $\xrightarrow{\Gamma = V_e - E \approx 0}$ asymptotic forms of the LTE for (1) the classical method (constant coefficients - (29)), (2) the four-stages method with vanished phase-lag and its first and second derivatives developed in [9] (with LTE given by (30)) and (3) the four-stages method with vanished phase-lag

and its derivatives up to order 3 developed in Section 3 (with LTE given by (27)), are the same and equal to $h^{16} \zeta_0$, where ζ_0 is given in the Appendix E.

2. **The Energy and the Potential are far from each other.** Therefore, $\Gamma \gg 0 \vee \Gamma \ll 0 \Rightarrow |\Gamma| \gg 0$.

Resultants:

For each family of methods the most accurate one is the scheme with asymptotic formula of LTE, given by (31) with the minimum power of Γ (i.e. minimum values for k) and the maximum value of p .

- Based on the achievements described above we obtain the following asymptotic forms of the LTE formulae for the schemes which are under evaluation.

4.1.4 Classical method

The Classical Method is the method (17) with constant coefficients.

$$LTE_{CL} = \frac{53}{32330691993600} h^{16} \left(\varepsilon(x) \Gamma^8 + \dots \right) + O(h^{18}). \tag{34}$$

4.1.5 P-stable method with vanished phase-lag and its first and second derivatives developed in [9]

$$LTE_{NM4SPS2DV} = \frac{53}{505167062400} h^{16} \left(\frac{d^2}{dx^2} \Xi(x) \varepsilon(x) \Gamma^6 + \dots \right) + O(h^{18}). \tag{35}$$

4.1.6 P-stable method with vanished phase-lag and its first, second and third derivatives developed in Section 3

$$\begin{aligned}
 LTE_{NM4SPS3DV} = & \frac{53}{404133649920} h^{16} \left[3 \left(\frac{d}{dx} \Xi(x) \right)^2 \varepsilon(x) \right. \\
 & + 11 \varepsilon(x) \frac{d^4}{dx^4} \Xi(x) + 2 \left(\frac{d}{dx} \varepsilon(x) \right) \left(\frac{d^3}{dx^3} \Xi(x) \right) \\
 & \left. + 4 \Xi(x) \varepsilon(x) \left(\frac{d^2}{dx^2} \Xi(x) \right) \right] \Gamma^5 + \dots + O(h^{18}). \tag{36}
 \end{aligned}$$

We present here the leading term in the asymptotic form of the Local Truncation Error. Consequently, the symbol \dots means that there are also terms for Γ^j $j = 0(1)5$.

The above analysis leads to the following theorem:

Theorem 3.

- *Classical Method (i.e., the method (17) with constant coefficients): For this method the error increases as the eighth power of Γ .*
- *P-Stable Tenth Algebraic Order Method with Vanished Phase-Lag and Its First and Second Derivatives Developed in [9]: For this method the error increases as the sixth power of Γ .*
- *P-Stable Method with Vanished Phase-Lag and Its First, Second and Third Derivatives Developed in Section 3: For this method the error increases as the fifth power of Γ .*

Consequently, for the numerical solution of the time independent radial Schrödinger equation, which is the scalar model for the local truncation error analysis, the newly introduced scheme is the most accurate one.

4.2 Stability analysis

Our analysis is based on the model equation:

$$\varepsilon'' = -\omega^2 \varepsilon. \tag{37}$$

Remark 10. *Observing the models (8) and (37) one can see that $\omega \neq \phi$, where ϕ is the frequency of the model (8) (phase-lag analysis) and ω is the frequency of the model (37) (stability analysis).*

If we apply the newly introduced algorithm (17) to the model (37), we obtain the difference equation:

$$\Omega_1(s, v) (\varepsilon_{n+1} + \varepsilon_{n-1}) + \Omega_0(s, v) \varepsilon_n = 0 \tag{38}$$

and the associated characteristic equation:

$$\Omega_1(s, v) (\lambda^2 + 1) + \Omega_0(s, v) \lambda = 0 \tag{39}$$

where the stability polynomials $\Omega_j(s, v)$, $j = 0, 1$ are given by:

$$\begin{aligned}\Omega_1(s, v) &= 1 + s^2 b_1 + s^4 b_1 c_5 + s^6 b_1 c_3 c_5 + s^8 b_1 c_1 c_3 c_5 \\ \Omega_0(s, v) &= a_1 + s^2 b_0 - s^4 b_1 c_4 - s^6 b_1 c_2 c_5 - s^8 b_1 c_0 c_3 c_5,\end{aligned}\tag{40}$$

where $s = \omega h$ and $v = \phi h$.

Substituting the coefficients $b_j, j = 0, 1$ and $c_k, k = 3(1)5$ given by (18) and the coefficients a_1 and $c_i, i = 0(1)2$ given by (26) into the stability polynomials (40), we obtain:

$$\begin{aligned}\Omega_1(s, v) &= -\frac{\Upsilon_{11}(s, v)}{85044960 \Upsilon_{12}(s, v)} \\ \Omega_0(s, v) &= \frac{\Upsilon_{13}(s, v)}{1020539520 \Upsilon_{12}(s, v)}\end{aligned}\tag{41}$$

where $\Upsilon_j(s, v), j = 7(1)9$ are given in the Appendix F.

Remark 11. *The conditions and definitions of P-stability and singularly almost P-stability, which are given in Section 2, are hold for problems with one frequency i.e. for problems with: $\omega = \phi$.*

In order the newly introduced algorithm (17) to satisfy the condition of a non zero interval of periodicity, the roots of its characteristic equation (39) must satisfy the relation:

$$|\lambda_{1,2}| \leq 1\tag{42}$$

4.2.1 Flowchart for the development of the $s - v$ domain for the newly introduced algorithm

Figure 3 presents the flowchart for the construction of the $s - v$ domain for the newly introduced scheme.

The procedure described in the flowchart of Figure 3 leads to the $s - v$ domain which is constructed in Figure 4.

Remark 12. *Remarking on the $s-v$ domain of Figure 4 leads to the following conclusions:*

1. *The newly introduced scheme is stable within the shadowed area of the domain.*
2. *The newly introduced scheme is unstable within the white area of the domain.*

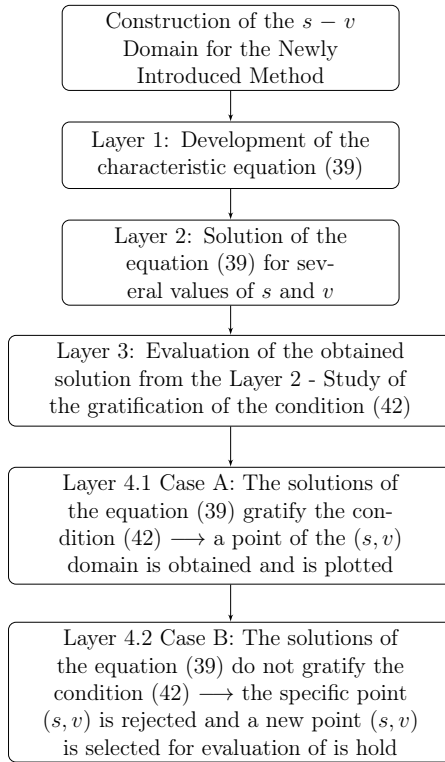


Figure 3. Flowchart for the development of the $s - v$ domain for the newly introduced algorithm

Remark 13. *Studying the above remarks, we obtain the following conclusions on the applicability of the newly introduced scheme:*

1. **Problems for which $\omega \neq \phi$.** *For these kind of problems, the most efficient methods are those with $s - v$ domain within the shadowed area of the Figure 4 excluding the area around the first diagonal.*
2. **Problems for which $\omega = \phi$** *(see the Schrödinger equation and related problems). For these kind of problems the most efficient methods are those with $s - v$ domain equal with the area around the first diagonal of the Figure 4.*

The interval of periodicity of the newly introduced scheme is determined as follows:

1. Substitution $s = v$ on the stability polynomials Ω_i , $i = 0, 1$ given by (41).

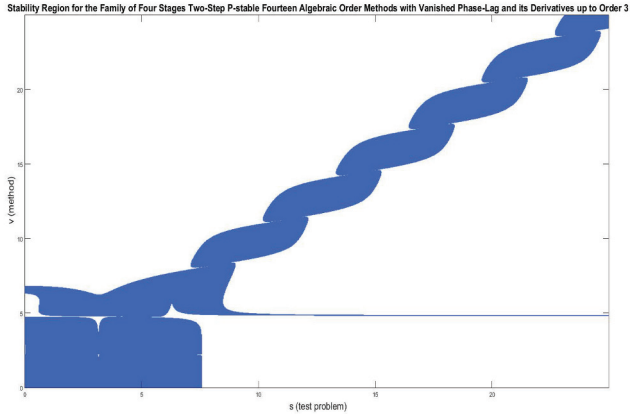


Figure 4. The plot of $s - v$ domain of the newly introduced scheme

2. Observation of the produced area around the first diagonal of the $s - v$ domain defined in Figure 4.

The above procedure leads us to the conclusion that the interval of periodicity of the newly introduced scheme is equal to $(0, \infty)$.

The above achievements lead to the following theorem:

Theorem 4. *The newly introduced scheme:*

- *is of four stages*
- *is of fourteen algebraic order,*
- *has eliminated the phase-lag and its derivatives up to order three and*
- *is P-stable i.e. has an interval of periodicity equals to: $(0, \infty)$.*

5 Numerical results

We apply the newly introduced method to the approximate solution of:

1. The one-dimensional time-independent Schrödinger equation and

2. The systems of coupled differential equations of the Schrödinger type.

in order to test its effectiveness

5.1 Radial time independent Schrödinger equation

The radial time-independent Schrödinger equation is expressed by the model:

$$\varepsilon''(r) = [l(l+1)/r^2 + V(r) - k^2] \varepsilon(r), \quad (43)$$

where

1. The function $\Theta(r) = l(l+1)/r^2 + V(r) \rightarrow$ *the effective potential*: $\Theta(r) \rightarrow 0$ as $r \rightarrow \infty$.
 2. $k^2 \in \mathbb{R} \rightarrow$ *the energy*.
 3. $l \in \mathbb{Z} \rightarrow$ *the angular momentum*.
 4. The function $V \rightarrow$ *the potential*.
- (43) \rightarrow boundary value problem \Leftrightarrow

$$\varepsilon(0) = 0$$

and an end point condition \rightarrow for large values of r from the physical considerations and characteristics of the specific problem.

The newly introduced scheme has its coefficients $a_1, c_j, j = 0(1)2$ dependent from the quantity $v = \phi h$, where ϕ is the frequency of the specific problem. Consequently, the determination during the integration of the previously mentioned coefficients is dependent on the determination of the frequency ϕ for the specific problem. In our numerical tests and for (43) and $l = 0$ we have:

$$\phi = \sqrt{|V(r) - k^2|} = \sqrt{|V(r) - E|}$$

where $V(r) \rightarrow$ the potential and $E = k^2 \rightarrow$ the energy.

5.1.1 Woods–Saxon potential

Observing the equation (43), we conclude that the determination of the value of the potential $V(r)$ is necessary in order to proceed with the integration of the problem. For our numerical tests we use the Wood–Saxon potential, the formula of which is given by:

$$V(r) = \frac{\Psi_0}{1 + \xi} - \frac{\Psi_0 \xi}{a(1 + \xi)^2} \tag{44}$$

with $\xi = \exp\left[\frac{r-X_0}{a}\right]$, $\Psi_0 = -50$, $a = 0.6$, and $X_0 = 7.0$.

The form of the Wood–Saxon potential for several values of r is presented in Figure 5.

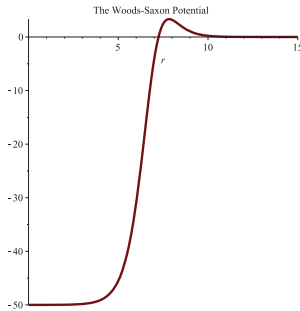


Figure 5. Form of the Woods–Saxon potential for several values of r .

For the Woods–Saxon potential and the procedure introduced in [21], [22] and [20], the following values of the frequency ϕ are used during the integration procedure:

$$\phi = \begin{cases} \sqrt{-50 + E} & \text{for } r \in [0, 6.5 - 2h] \\ \sqrt{-37.5 + E} & \text{for } r = 6.5 - h \\ \sqrt{-25 + E} & \text{for } r = 6.5 \\ \sqrt{-12.5 + E} & \text{for } r = 6.5 + h \\ \sqrt{E} & \text{for } r \in [6.5 + 2h, 15]. \end{cases}$$

Some examples are given below:

1. On $r = 6.5 - h$, the value of ϕ is approximated by the value: $\sqrt{-37.5 + E}$. Consequently, $v = \phi h = \sqrt{-37.5 + E} h$.
2. On $r = 6.5 - 3h$, the value of ϕ is approximated by the value: $\sqrt{-50 + E}$. Consequently, $v = \phi h = \sqrt{-50 + E} h$.

Remark 14. We note here that the potential $V(r)$ is a user defined function. There are a lot of potentials which are of great interest in several disciplines of Chemistry. For the most of them, their eigenenergies are unknown. We selected the Woods–Saxon potential since for this potential the eigenenergies are known.

5.1.2 The resonance problem of the radial Schrödinger equation

For the problem of our interest (43) (as this presented in the paragraphs above), it is noted that from theoretical point of view the integration interval is equal to $[0, \infty)$. The approximate solution of the problem (43) requests the interval $[0, \infty)$ to be approximated by an interval $[0, i_a]$, where $i_a \in \mathbb{R}$. For our tests we determine $i_a = 15$. We will use for our applications a wide range of energies: $E \in [1, 1000]$.

Since $V(r) \rightarrow 0$ faster than the term $\frac{l(l+1)}{r^2} \Rightarrow$ New form for the equation (43):

$$\varepsilon''(r) + \left(k^2 - \frac{l(l+1)}{r^2} \right) \varepsilon(r) = 0 \quad (45)$$

when $r \rightarrow \infty$. The solutions of the model (45) are given by $kr j_l(kr)$ and $kr n_l(kr)$, which are linearly independent, with $j_l(kr)$ and $n_l(kr)$ represent the spherical Bessel and Neumann functions respectively (see [85]).

The asymptotic form of the solution of the model (43) (i.e. in the case where $r \rightarrow \infty$) is given by:

$$\begin{aligned} \varepsilon(r) &\approx K kr j_l(kr) - LN kr n_l(kr) \\ &\approx KM \left[\sin \left(kr - \frac{l\pi}{2} \right) + \tan \delta_l \cos \left(kr - \frac{l\pi}{2} \right) \right] \end{aligned}$$

where δ_l is the phase shift and $K, LN, KM \in \mathbb{R}$. The formula:

$$\tan \delta_l = \frac{\varepsilon(r_2) S(r_1) - \varepsilon(r_1) S(r_2)}{\varepsilon(r_1) C(r_1) - \varepsilon(r_2) C(r_2)}$$

gives a direct procedure in order to compute the phase shift. In this formula r_1 and r_2 are distinct points in the asymptotic region (we chosen $r_1 = 15$ and $r_2 = r_1 - h$) with $S(r) = kr j_l(kr)$ and $C(r) = -kr n_l(kr)$. The problem described above is an initial–value one. Therefore, it is necessary to compute the values of ε_j , $j = 0, 1$ before starting the application of a two–step scheme. The value ε_0 is determined by the initial condition of the problem. The value ε_1 is computed using the high order Runge–Kutta–Nyström methods (see [23] and [24]). The values ε_i , $i = 0, 1$ are the basis in order to

compute the phase shift δ_l at the point r_2 of the asymptotic region. We note that ε_j is the approximation of the function ε at the point x_j .

The numerical solution of the above problem leads to two possible results:

- the phase-shift δ_l or
- The energies E , for $E \in [1, 1000]$, for which $\delta_l = \frac{\pi}{2}$.

In our numerical tests we chosen the second problem, which is known as **the resonance problem**.

The boundary conditions are:

$$\varepsilon(0) = 0 \quad , \quad \varepsilon(r) = \cos\left(\sqrt{Er}\right) \quad \text{for large } r.$$

For the computation of the the positive eigenenergies of the resonance problem and for comparison purposes we use the methods presented in Table 1.

Table 1. Numerical Methods used in our numerical test for comparison purposes. *AO*: Algebraic order, *PL*: Vanished Phase-Lag or Minimal Phase-Lag. *DPL*: Maximum order of the Derivative of the phase-lag which is vanished. Notes: (1) The notation *EXP* in the column *PL* means: exponentially-fitted method. (2) The notation *P* near to the algebraic order means: P-stable method

Method	AO	PL	DPL	Reference
QT8	8	–	–	[25]
QT10	10	–	–	[25]
QT12	12	–	–	[25]
MCR4	4	<i>YES</i>	–	[26]
RA	4	<i>EXP</i>	–	[27]
MCR6	6	<i>YES</i>	–	[28]
NMPF1	4	<i>YES</i>	–	[15]
NMPF2	4	<i>YES</i>	–	[15]
NMPC2	4	<i>YES</i>	1	[29] (Case 2)
NMPC1	4	<i>YES</i>	1	[29] (Case 1)
NM2SH2DV	10	<i>YES</i>	2	[1]
WPS2S	4 <i>P</i>	–	–	[84]
WPS4S	6 <i>P</i>	–	–	[84]
WPS6S	8 <i>P</i>	–	–	[84]
NM3SPS2DV	10	<i>YES</i>	2	[6]
NM3SPS3DV	10	<i>YES</i>	3	[7]
NM4SPS2DV	14	<i>YES</i>	2	[9]
NM4SPS3DV	14	<i>YES</i>	3	Section 3

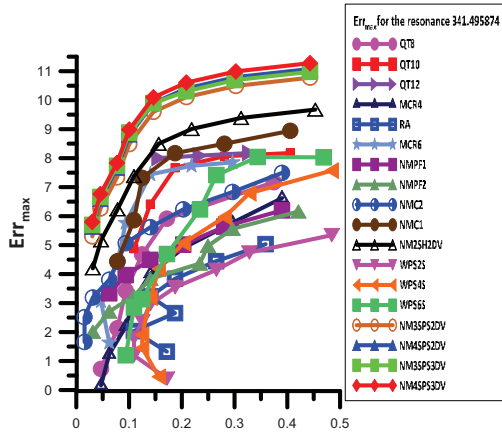


Figure 6. Accuracy (Digits) for several values of *CPU* Time (in Seconds) for the eigenvalue $E_2 = 341.495874$. The nonexistence of a value of Accuracy (Digits) indicates that for this value of *CPU*, Accuracy (Digits) is less than 0.

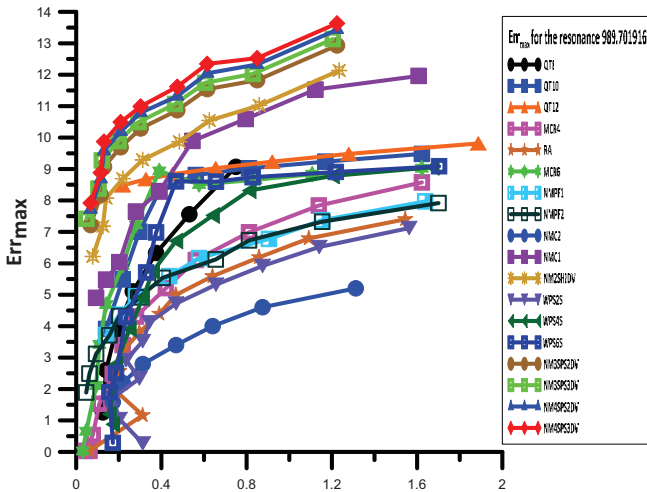


Figure 7. Accuracy (Digits) for several values of *CPU* Time (in Seconds) for the eigenvalue $E_3 = 989.701916$. The nonexistence of a value of Accuracy (Digits) indicates that for this value of *CPU*, Accuracy (Digits) is less than 0.

The maximum absolute errors Err_{max} , which are defined by:

$$Err_{max} = \max |\log_{10}(Err)| \quad (46)$$

where

$$Err = |E_{calculated} - E_{accurate}|. \quad (47)$$

is presented in Figures 6 and 7.

In order to define the quantity Err , we consider two values for the specific eigenenergy:

1. The computed eigenenergies notated as $E_{calculated}$ which are determined using each of the numerical methods under evaluation.
2. The accurate eigenenergies (or as also called **reference values** for the eigenenergies) notated as $E_{accurate}$ which are determined using the well known two-step method of Chawla and Rao [28].

In Figures 6 and 7 we present the following:

- the maximum absolute errors Err_{max} for the eigenenergies $E_2 = 341.495874$ and $E_3 = 989.701916$, respectively, for several values of CPU time (in seconds). We use for comparison purposes the numerical methods presented in Table 1.
- the needed CPU time (in seconds) (as mentioned above).

The symbols E_2 and E_3 are used for the eigenenergies in our numerical tests since it is known that the Woods–Saxon potential has also the eigenenergies E_0 and E_1 . We chose the eigenenergies E_2 and E_3 because for these eigenenergies the solution has stiffer behavior and therefore the newly introduced algorithm can show its efficiency more effectively.

5.1.3 Conclusions

Figures 6 and 7 lead us to the following conclusions:

- **Method QT10** is more efficient than **Method MCR4** and **Method QT8**.
- **Method QT10** is more efficient than **Method MCR6** for large CPU time and less efficient than **Method MCR6** for small CPU time.
- **Method QT12** is more efficient than **Method QT10**

- **Method NMPF1** is more efficient than **Method RA**, **Method NMPF2** and **Method WPS2S**
- **Method WPS4S** is more efficient than **Method MCR4**, **Method NMPF1** and **Method NMC2**.
- **Method WPS6S** is more efficient than **Method WPS4S**.
- **Method NMC1**, is more efficient than all the other methods mentioned above.
- **Method NM2SH2DV**, is more efficient than all the other methods mentioned above.
- **Method NM3SPS2DV**, is more efficient than all the other methods mentioned above.
- **Method NM3SPS23DV**, is more efficient than all the other methods mentioned above.
- **Method NM4SPS2DV**, is more efficient than all the other methods mentioned above.
- **Method NM4SPS3DV**, is the most efficient one.

5.2 Error estimation

For the second test, which is the approximate solution of systems of coupled differential equations arising from the Schrödinger equation, we need variable-step schemes.

Definition 10. *We call a method as a variable-step scheme if its stepsize or step length is changing during the integration procedure.*

Definition 11. *A variable-step technique for changing the step length during the integration is called Local Truncation Error Estimation Procedure and we symbolize it as *LTERRSTR*.*

In the [15]– [84] and references therein one can find the bibliography on the construction of numerical schemes of constant or variable step length for the numerical solution of the Schrödinger equation and related problems.

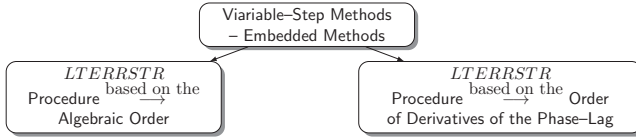


Figure 8. Categories of *LTERRSTR* Procedures used for the Construction of Embedded Schemes for the Problems with Oscillatory and/or Periodical Solutions

The categories of the *LTERRSTR* procedures are shown in Figure 8.

In order to obtain changing of the stepsize during the integration, it is necessary to estimate the local truncation error (*LTE*) on the lower order solution ε_{n+1}^L . The estimation of the local truncation error (*LTE*) is based on the relation:

$$LTE = | \varepsilon_{n+1}^H - \varepsilon_{n+1}^L | \tag{48}$$

where ε_{n+1}^L and ε_{n+1}^H are

- ***LTERRSTR* Technique** $\xrightarrow{\text{based on the}}$ **algebraic order of the numerical methods.** For this technique: $\xrightarrow{\text{based on the}}$ ε_{n+1}^L : numerical scheme of lower algebraic order and ε_{n+1}^H : numerical scheme of higher algebraic order.

Definition 12. *We consider that we have two numerical schemes (symbolized as ε_{n+1}^L and ε_{n+1}^H) of the same algebraic order. The scheme ε_{n+1}^L has vanished the phase-lag and its derivatives up to order p . The scheme ε_{n+1}^H has vanished the phase-lag and its derivatives up to order s , where $p < s$. Then we call higher order the scheme ε_{n+1}^H .*

- ***LTERRSTR* Technique** $\xrightarrow{\text{based on the}}$ **derivatives of the phase-lag.** Let us consider the schemes of the above definition. For this procedure ε_{n+1}^L denotes the lower order numerical method and ε_{n+1}^H denotes the higher order numerical method.

In our numerical tests, the estimation of the local truncation error (error control procedure) is done using the *LTERRSTR* procedure based on the algebraic order of the numerical schemes (first methodology), as follows:

- $\varepsilon_{n+1}^L \xrightarrow{\text{based on the}}$ 10th algebraic order method obtained in [7]

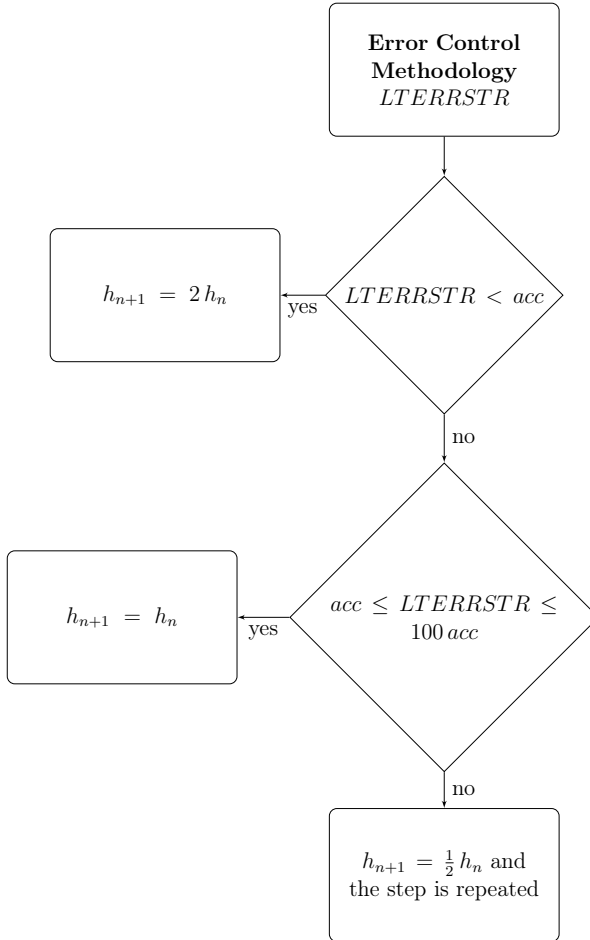


Figure 9. Flowchart for the Local Truncation Error Control Methodology *LERRSTR*. The parameter *acc* is determined by the user

- $\varepsilon_{n+1}^H \longrightarrow$ 14th algebraic order method developed in Section 3.

In Figure 9 the variable-step procedure used in our paper is presented, where:

- h_n is determined as the stepsize which is used during the n^{th} step of the integration procedure and
- *acc* is determined as the requested accuracy for the local truncation error *LTE* which is defined by the user.

Remark 15. *The local extrapolation procedure is also used: the local truncation error estimation is based on the lower order solution ε_{n+1}^L while the approximation of the solution at each point of the integration domain is done via the higher order solution ε_{n+1}^H .*

5.3 The system of coupled differential equations arising from the Schrödinger equation

The model of the close-coupling Schrödinger equations is described by the following system of equations:

$$\left[\frac{d^2}{dx^2} + k_i^2 - \frac{l_i(l_i + 1)}{x^2} - V_{ii} \right] \varepsilon_{ij} = \sum_{m=1}^N V_{im} \varepsilon_{mj}$$

for $1 \leq i \leq N$ and $m \neq i$.

We can find models like the above in several scientific disciplines like: quantum chemistry, mathematical chemistry, material science, theoretical physics, quantum physics, atomic physics, physical chemistry, chemical physics, electronics, etc.

The boundary conditions, are given by (see for details [30]):

$$\varepsilon_{ij} = 0 \text{ at } x = 0$$

$$\varepsilon_{ij} \sim k_i x j_{l_i}(k_i x) \delta_{ij} + \left(\frac{k_i}{k_j} \right)^{1/2} K_{ij} k_i x n_{l_i}(k_i x) \quad (49)$$

The study described in [30] leads to the new formulae of the asymptotic condition (49):

$$\varepsilon \sim \mathbf{M} + \mathbf{N}\mathbf{K}'.$$

where the matrix \mathbf{K}' and diagonal matrices \mathbf{M} , \mathbf{N} are give by :

$$K'_{ij} = \left(\frac{k_i}{k_j} \right)^{1/2} K_{ij}$$

$$M_{ij} = k_i x j_{l_i}(k_i x) \delta_{ij}$$

$$N_{ij} = k_i x n_{l_i}(k_i x) \delta_{ij}$$

In our tests we solved the rotational excitation of a diatomic molecule by neutral particle impact. We can find this problem in several disciplines like quantum chemistry, theoretical chemistry, theoretical physics, quantum physics, material science, atomic physics,

molecular physics, in technical applications in the analysis of gas dynamics and stratification of chemically reacting flows, dispersed flows, including with nano-sized particles etc (see [10], [11–14], [86] - [99]).

Using the denotations:

- quantum numbers (j, l) which denote the entrance channel (see for details in [30]),
- quantum numbers (j', l') which denote the exit channels and
- $J = j + l = j' + l'$ which denote the total angular momentum.

we have:

$$\left[\frac{d^2}{dx^2} + k_{j'j}^2 - \frac{l'(l'+1)}{x^2} \right] \varepsilon_{j'l'}^{Jjl}(x) = \frac{2\mu}{\hbar^2} \sum_{j''} \sum_{l''} \langle j'l'; J | V | j''l''; J \rangle \varepsilon_{j''l''}^{Jjl}(x)$$

where

$$k_{j'j} = \frac{2\mu}{\hbar^2} \left[E + \frac{\hbar^2}{2I} \{j(j+1) - j'(j'+1)\} \right].$$

and E determines the kinetic energy of the incident particle in the center-of-mass system, I determines the moment of inertia of the rotator, μ determines the reduced mass of the system, Jjl determines the angular momentum of the quantum numbers (j, l) and j'' and l'' determine the quantum numbers.

The following potential V is used during our numerical experiments (see [30]):

$$V(x, \hat{\mathbf{k}}_{j'j} \hat{\mathbf{k}}_{jj}) = V_0(x) P_0(\hat{\mathbf{k}}_{j'j} \hat{\mathbf{k}}_{jj}) + V_2(x) P_2(\hat{\mathbf{k}}_{j'j} \hat{\mathbf{k}}_{jj})$$

and consequently, the coupling matrix has elements of the form:

$$\langle j'l'; J | V | j''l''; J \rangle = \delta_{j'j''} \delta_{l'l''} V_0(x) + f_2(j'l', j''l''; J) V_2(x)$$

where f_2 coefficients are determined from formulae described by Bernstein et al. [31] and $\hat{\mathbf{k}}_{j'j}$ determines a unit vector parallel to the wave vector $\mathbf{k}_{j'j}$ and P_i , $i = 0, 2$ determine the Legendre polynomials (see for details [32]). We note also that $V_0(x)$ and $V_2(x)$ determine the potential functions defined by the user. The above study leads to the following new formulae of the boundary conditions:

$$\varepsilon_{j'l'}^{Jjl}(x) = 0 \text{ at } x = 0 \tag{50}$$

$$\varepsilon_{j'l'}^{Jj}(x) \sim \delta_{jj'} \delta_{ll'} \exp[-i(k_{jj}x - 1/2l\pi)] - \left(\frac{k_i}{k_j}\right)^{1/2} S^J(jl; j'l') \exp[i(k_{j'j}x - 1/2l'\pi)]$$

where S matrix. For K matrix of (49) the following formula is used:

$$\mathbf{S} = (\mathbf{I} + i\mathbf{K})(\mathbf{I} - i\mathbf{K})^{-1}.$$

Our newly introduced methods are applied to the above described problem using the methodology fully described in [30].

We use the following parameters for the \mathbf{S} matrix for our numerical tests:

$$\frac{2\mu}{\hbar^2} = 1000.0 \quad ; \quad \frac{\mu}{I} = 2.351 \quad ; \quad E = 1.1$$

$$V_0(x) = \frac{1}{x^{12}} - 2\frac{1}{x^6} \quad ; \quad V_2(x) = 0.2283V_0(x).$$

For our tests we use (see for details in [30]):

- $J = 6$ and
- $j = 0$ for the excitation of the rotator state to levels up to $j' = 2, 4$ and 6 .

The above values lead to systems of **four, nine and sixteen coupled differential equations of the Schrödinger type**, respectively. The potential is considered infinite for x less than x_0 (see for details in [32] and [30]). Therefore, the boundary condition (50) can be written now as

$$\varepsilon_{j'l'}^{Jj}(x_0) = 0.$$

For our numerical test and for comparison purposes we use the following methods:

- the Iterative Numerov method of Allison [30] which is indicated as **ALGRT I**²,
- the variable-step method of Raptis and Cash [33] which is indicated as **ALGRT II**,
- the embedded Runge-Kutta Dormand and Prince method 5(4) (5(4) means: Runge-Kutta method of variable step which uses the fourth algebraic order part in order to control the error of the the fifth algebraic order part) which is developed in [24] which is indicated as **ALGRT III**,

²We note here that Iterative Numerov method developed by Allison [30] is one of the most well-known methods for the numerical solution of the coupled differential equations arising from the Schrödinger equation

- the embedded Runge–Kutta method ERK4(2) developed in Simos [34] which is indicated as **ALGRT IV**,
- the embedded two-step method developed in [1] which is indicated as **ALGRT V**,
- the new developed embedded two-step method with error control based on the algebraic order of the method developed in [6] which is indicated as **ALGRT VI**.
- the new developed embedded two-step method with error control based on the algebraic order of the method developed in [9] which is indicated as **ALGRT VII**.
- the new developed embedded two-step method with error control based on the algebraic order of the method developed in this paper which is indicated as **ALGRT VIII**.

In Table 2 we present:

- the real time of computation required by the numerical algorithms I-VIII mentioned above in order to calculate the square of the modulus of the **S** matrix for the sets of 4, 9 and 16 of systems of coupled differential equations respectively,
- the maximum error on the computation of the square of the modulus of the **S** matrix.

All computations were carried out on a x86-64 compatible PC using double-precision arithmetic data type (64 bits) according to IEEE[©] Standard 754 for double precision.

Table 2. Coupled Differential Equations. Real time of computation (in seconds) (RTC) and maximum absolute error (MErr) to calculate $|S|^2$ for the variable-step methods Method I - Method VIII. $acc=10^{-6}$. Note that hmax is the maximum stepsize. N indicates the number of equations of the set of coupled differential equations

Method	N	hmax	RTC	MErr
Method I	4	0.014	3.25	1.2×10^{-3}
	9	0.014	23.51	5.7×10^{-2}
	16	0.014	99.15	6.8×10^{-1}
Method II	4	0.056	1.55	8.9×10^{-4}
	9	0.056	8.43	7.4×10^{-3}
	16	0.056	43.32	8.6×10^{-2}
Method III	4	0.007	45.15	9.0×10^0
	9			
	16			
Method IV	4	0.112	0.39	1.1×10^{-5}
	9	0.112	3.48	2.8×10^{-4}
	16	0.112	19.31	1.3×10^{-3}
Method V	4	0.448	0.20	1.1×10^{-6}
	9	0.448	2.07	5.7×10^{-6}
	16	0.448	11.18	8.7×10^{-6}
Method VI	4	0.896	0.04	3.8×10^{-8}
	9	0.896	0.55	5.6×10^{-8}
	16	0.896	8.45	6.5×10^{-8}
Method VII	4	0.896	0.01	1.2×10^{-8}
	9	0.896	0.39	1.9×10^{-8}
	16	0.896	7.12	2.2×10^{-8}
Method VIII	4	0.896	0.01	9.8×10^{-9}
	9	0.896	0.37	1.1×10^{-8}
	16	0.896	7.12	1.5×10^{-8}

6 Conclusions

A new P-stable four-stages fourteen algebraic order two-step method with zeroing phase-lag and its derivatives up to order three was introduced in this paper.

The creation was done using the following levelnesses:

1. 1st Levelness: Satisfaction of the P-stability properties.
2. 2nd Levelness: Satisfaction of the property for the zeroing of the phase-lag.
3. 3rd Levelness: Satisfaction of the properties for the zeroing of the derivatives up to order three of the phase-lag.

The above methodology for the creation of newly obtained methods was first introduced by Medvedev and Simos [6].

We have also analyzed the newly introduced method using the following levels:

- 1st Levelness: Determination of the local truncation error (*LTE*).
- 2nd Levelness: Determination of the asymptotic form of the *LTE*
- 3rd Levelness: Comparison of the asymptotic form of the *LTE* of the newly introduced algorithm with the asymptotic forms of the *LTE* of similar algorithms.
- 4th Levelness: Study of the stability and the interval of periodicity properties of the the newly introduced algorithm.
- 5th Levelness: Evaluation of the computational effectiveness of the the newly introduced algorithm.

The theoretical, computational and numerical results obtained in this paper lead to the conclusion that the the newly introduced algorithm is more efficient for the numerical solution of the Schrödinger equation and related problems than other well known and recently created algorithms of the literature.

Appendix A: Formulae for the $\Upsilon_i(v)$, $i = 0(1)4$

$$\begin{aligned}\Upsilon_0 &= 4694 \cos(v) v^8 c_1 - 2347 v^8 c_0 \\ &+ 4694 \cos(v) v^6 - 173838 v^6 c_2 \\ &+ 347676 \cos(v) v^4 - 347676 v^4 + 14174160 \cos(v) v^2 \\ &+ 70870800 v^2 + 170089920 \cos(v) \\ &+ 85044960 a_1 \\ \Upsilon_1 &= 6027204351168000 v - 59136183025920 v^3 \\ &- 332667535200 v^7 - 7232645221401600 \sin(v) \\ &- 798402084480 v^7 c_0 + 815995572 v^9 - 14784045756480 v^5 \\ &- 2863208668320 \sin(v) v^6 - 44352137269440 v^5 c_2 \\ &- 1205440870233600 \sin(v) v^2 - 5508409 v^{13} c_0 \\ &- 63486403764 \sin(v) v^8 - 79794794439360 \sin(v) v^4 \\ &- 399201042240 \sin(v) v^8 c_1 - 33266753520 \sin(v) v^{10} c_1 \\ &- 11016818 \sin(v) v^{14} c_1 + 407997786 v^{13} c_1 c_2 \\ &- 798402084480 v^7 a_1 c_1 - 815995572 \sin(v) v^{12} c_1 \\ &- 5508409 \sin(v) v^{16} c_1^2 - 5508409 \sin(v) v^{12} \\ &- 29568091512960 v^3 a_1 - 602720435116800 v a_1 \\ &- 30219650244 v^9 c_2 - 815995572 \sin(v) v^{10}\end{aligned}$$

$$\begin{aligned} & - 2464007626080 v^7 c_2 - 598801563360 v^5 a_1 - 815995572 v^{11} c_0 \\ & + 1631991144 v^{11} c_1 - 49900130280 v^9 c_0 - 499001302800 v^9 c_1 \\ \Upsilon_2 = & - 2872712411226 v^{16} c_0 - 14351287847755098240 v^{10} c_1 \\ & - 561835147647533760 \cos(v) v^{12} c_1 - 20159852233641120 \cos(v) v^{14} c_1 \\ & - 447007768902324 \cos(v) v^{16} c_1 - 12928235923 v^{18} c_0 \\ & - 329892163135164 \cos(v) v^{14} - 24007788523551672 \cos(v) v^{12} \\ & - 2872712411226 \cos(v) v^{16} - 1204342384201276320 \cos(v) v^{10} \\ & - 12928235923 \cos(v) v^{18} + 37016968351902739200 v^6 a_1 \\ & - 12928235923 \cos(v) v^{24} c_1^3 - 475300513369627545600 v^6 a_1 c_1 \\ & - 38784707769 \cos(v) v^{22} c_1^2 + 1040944661713756800 v^{10} a_1 c_1 \\ & + 4243754583657388800 v^8 a_1 c_1 + 24828508422637920 v^{12} a_1 c_1 \\ & + 1596115147961093760 v^{12} c_1 c_2 + 16864647230471040 v^{14} c_0 c_1 \\ & + 78070849628531760 v^{14} c_1 c_2 + 16864647230471040 v^{14} a_1 c_1^2 \\ & + 851106229472016 v^{16} c_1 c_2 - 50925055003888665600 \cos(v) v^8 c_1 \\ & + 23661805932932328 v^{12} c_2 - 45876483175002480 v^{12} c_0 \\ & + 212776557368004 v^{14} c_2 + 11391510748516416 v^{14} c_1 \\ & + 512583352956908513280000 - 2872712411226 \cos(v) v^{20} c_1^2 \\ & - 425553114736008 v^{14} c_0 - 19151416074840 v^{18} c_1^2 \end{aligned}$$

$$\begin{aligned} &+ 5270732343934644787200 v^2 a_1 + 688356159979065177600 v^4 a_1 \\ &+ 329632476209356320 v^{10} + 4045704563817336 v^{12} \\ &- 5745424822452 v^{14} - 8487509167314777600 \cos(v) v^{10} c_1 \\ &- 51258335295690851328000 a_1 - 615100023548290215936000 \cos(v) \\ &- 13201740089979119078400 v^4 - 407021351380317273600 v^6 \\ &- 143233541199203264409600 v^2 + 38784707769 v^{20} c_0 c_1 \\ &- 2872712411226 v^{20} c_1^2 c_2 - 117115605767160 \cos(v) v^{18} c_1^2 \\ &- 5745424822452 \cos(v) v^{18} c_1 - 38784707769 \cos(v) v^{20} c_1 \\ &+ 957570803742 v^{18} c_1 c_2 + 2510862923634024960 v^8 \\ &+ 9575708037420 v^{18} c_0 c_1 + 819809240370120 v^{16} c_0 c_1 \\ &+ 936850195542381120 v^8 a_1 + 375896683396634400 v^{12} c_1 \\ &+ 9837710884441440 v^{10} a_1 - 17236274467356 v^{16} c_1 \\ &- 1781187154997182732800 v^6 c_2 - 1035540006778525248000 \cos(v) v^6 \\ &- 16586509563916746854400 \cos(v) v^4 \\ &- 153775005887072553984000 \cos(v) v^2 \\ &- 594125641712034432000 v^8 c_1 - 55168809587546054400 v^8 c_0 \\ &- 2392797873552166080 v^{10} c_0 + 86154026645887200 v^{10} c_2 \\ &- 1405387269205920 \cos(v) v^{16} c_1^2 - 475300513369627545600 v^6 c_0 \end{aligned}$$

$$\begin{aligned} & - 18859628699970170112000 v^4 c_2 + 8198092403701200 v^{16} c_1^2 \\ & - 52387857499917139200 v^8 c_2 - 42391524755918257920 \cos(v) v^8 \\ \Upsilon_3 = & 397971634408560605352960 \sin(v) v^{16} c_1 \\ & + 25446708584454311462814105600 v^7 \\ & + 52311156898663399482668482560000 \sin(v) \\ & + 206772616050921680284901376000 v^5 \\ & - 8342534154341464197120 v^{13} + 23190744096195662572185600 v^{11} \\ & + 1174242622320956509755033600 v^9 \\ & - 1499813149818361192481931264000 v^3 \\ & - 46158896938332270424946245632000 v \\ & - 726085249030530738720 v^{19} c_1 c_2 \\ & + 8989674705529896 \sin(v) v^{28} c_1^3 + 121370278845124 \sin(v) v^{30} c_1^3 \\ & + 40159090975626570582835200 v^{13} a_1 c_1^2 - 1997546320570821552 v^{19} c_2 \\ & + 121370278845124 \sin(v) v^{26} c_1 \\ & - 242531478884996638982701056000 v^5 a_1 c_1 \\ & + 366493768980699360 \sin(v) v^{26} c_1^3 \\ & + 239042208188253396326400 \sin(v) v^{16} c_1^2 \\ & - 969561488447461644134400 v^{13} a_1 c_1 \end{aligned}$$

$$\begin{aligned} &+ 507054163694557704825600 \sin(v) v^{14} \\ &- 49839181269260619075840 v^{19} c_1^2 c_2 + 182055418267686 \sin(v) v^{28} c_1^2 \\ &- 54725375511344993495040 v^{15} a_1 c_1 + 26969024116589688 v^{27} c_1^3 c_2 \\ &+ 11306366302881582092160 \sin(v) v^{18} c_1 - 7990185282283286208 v^{21} c_1 c_2 \\ &- 857595419414836502400 v^{19} a_1 c_1^2 + 19975463205708215520 v^{21} c_0 c_1 \\ &+ 30342569711281 \sin(v) v^{32} c_1^4 \\ &+ 1169025377658267429780480000 v^9 a_1 c_1 \\ &+ 9582339380693747882256 \sin(v) v^{16} \\ &+ 9721649583636795028224000 \sin(v) v^{14} c_1 \\ &+ 2514169558141543389562675200 v^{11} c_1 c_2 \\ &+ 32971528712377724320051200 v^{11} a_1 c_1 \\ &+ 323628289399076256 v^{23} c_1^2 - 364110836535372 v^{27} c_0 c_1^2 \\ &+ 135152697502160071776 \sin(v) v^{18} + 1365266929266110136 \sin(v) v^{20} \\ &+ 8989674705529896 \sin(v) v^{22} + 30342569711281 \sin(v) v^{24} \\ &+ 4397925227768392320 \sin(v) v^{24} c_1^3 \\ &+ 94630346384711417280 \sin(v) v^{22} c_1^2 \\ &+ 225385118659103096736 \sin(v) v^{20} c_1 \\ &+ 40159090975626570582835200 v^{13} c_0 c_1 \end{aligned}$$

$$\begin{aligned} & - 2117350838236562248320 v^{21} c_1^2 c_2 - 395813270499155308800 v^{21} a_1 c_1^3 \\ & - 395813270499155308800 v^{21} c_0 c_1^2 + 157245105058354146113280 v^{17} c_0 c_1 \\ & + 39840368031375566054400 \sin(v) v^{18} c_1^2 \\ & + 2637254183057523469440 \sin(v) v^{20} c_1^2 \\ & + 3097027627512919632 \sin(v) v^{22} c_1 + 26969024116589688 \sin(v) v^{24} c_1 \\ & + 2098254467227508856 \sin(v) v^{24} c_1^2 \\ & + 236072258980426609348608000 v^{13} c_1 c_2 \\ & - 28339926604089371631360 v^{17} a_1 c_1^2 - 672882559848564024960 v^{17} a_1 c_1 \\ & + 1443639755267837136801792000 \sin(v) v^{10} c_1 \\ & + 5774559021071348547207168000 v^7 a_1 c_1 \\ & - 242531478884996638982701056000 v^5 c_0 \\ & + 63620455834621388102400 v^{17} c_1 c_2 \\ & + 796807360627511321088000 v^{15} a_1 c_1^2 \\ & + 5774559021071348547207168000 \sin(v) v^8 c_1 \\ & + 4143398275263058869657600 v^{15} c_0 c_1 \\ & + 7551740404579062085954560 v^{15} c_1 c_2 \\ & - 37534633636963765556846592000 v^7 c_0 \\ & + 233792957883787262648303616000 \sin(v) v^6 \end{aligned}$$

$$\begin{aligned} & - 641566547361526047347294208000 v^5 c_2 \\ & + 2607342569018659010009382912000 \sin(v) v^4 \\ & + 17437052299554466494222827520000 \sin(v) v^2 \\ & - 433091926580351141040537600000 v^7 c_1 \\ & - 330727550462939617827840 v^{13} c_0 - 62902458190619933453568000 v^{11} c_0 \\ & + 1009598653562286849552691200 v^{11} c_1 - 2321173784687806124671795200 v^9 c_0 \\ & - 13230558249057572806320537600 v^9 c_1 + 1808233538964379954089062400 v^9 c_2 \\ & - 9414424892965909397188608000 v^7 c_2 + 2134693149176787697225728000 v^5 a_1 \\ & - 6415665473615260473472942080000 v^3 c_2 - 15392738297189373120 v^{23} c_0 c_1^2 \\ & - 39582199316502668220595200 v^9 a_1 + 113183486507397084302684160 v^{11} c_2 \\ & + 2459086031046110514048000 v^{13} c_2 - 1415103977614145581002240 v^{11} a_1 \\ & + 65675878440210232749434880 v^{13} c_1 - 25408210058838746979840 v^{13} a_1 \\ & + 10446087869229892239360 v^{15} c_2 + 16890785733081830169600 v^{15} c_0 \\ & + 797578507723905594086400 v^{15} c_1 - 184712859566272477440 v^{15} a_1 \\ & + 364110836535372 v^{25} c_0 c_1 + 2584130544281539693440 v^{19} c_0 c_1 \\ & - 26969024116589688 v^{25} c_1^2 c_2 + 26969024116589688 \sin(v) v^{26} c_1^2 \\ & - 58969157988246547104 v^{17} - 134845120582948440 v^{25} c_0 c_1^2 \\ & - 325816066216361931840 v^{21} c_1^2 + 215752192932717504 v^{21} c_1 \end{aligned}$$

$$\begin{aligned}
& - 232872004165848493824 v^{19} c_1 - 6514925656112499225600 v^{15} \\
& + 53938048233179376 v^{19} + 107876096466358752 v^{23} c_0 c_1 \\
& - 19975463205708215520 v^{23} c_1^2 c_2 - 6514925656112499225600 v^{19} c_1^2 \\
& + 898065013628723472 v^{19} c_0 + 155714151786050419469107200 \sin(v) v^{12} c_1 \\
& - 259228248788074884192 v^{17} c_2 + 33465909146355475485696000 v^{15} c_1^2 \\
& - 13385434668398335738944 v^{17} c_1 + 1023242817773257776414720 v^{17} c_1^2 \\
& + 274695941072955239712 v^{17} c_0 + 621800118802753220852121600 \sin(v) v^{10} \\
& + 14188415986835147446547558400 \sin(v) v^8 \\
& + 20376682515327609262471680 \sin(v) v^{12} \\
& + 191676239138071100509544448000 v^3 a_1 \\
& + 3076129980165564528861118464000 v a_1 \\
& + 269690241165896880 v^{25} c_1^3 - 153927382971893731200 v^{23} c_1^3 \\
& - 517831106839807794556723200 v^7 a_1 \\
\Upsilon_4 = & 2347 v^8 c_1 + 2347 v^6 + 173838 v^4 + 7087080 v^2 + 85044960.
\end{aligned}$$

Appendix B: Formulae for the $\Upsilon_j(v)$, $j = 5(1)10$

$$\begin{aligned}
\Upsilon_5 = & -2347 v^9 \cos(2v) - 11735 v^9 \\
& - 354717 v^7 \cos(2v) + 1390704 \sin(v) v^6 \\
& + 1390704 v^6 \sin(2v) - 1731339 v^7
\end{aligned}$$

$$\begin{aligned} & - 12516336 \cos(v) v^5 - 22304268 v^5 \cos(2v) \\ & - 871310160 \sin(v) v^4 + 180520200 v^4 \sin(2v) \\ & - 92746836 v^5 + 9354945600 \cos(v) v^3 \\ & - 233873640 v^3 \cos(2v) + 17859441600 \sin(v) v^2 \\ & + 5868102240 v^2 \sin(2v) + 63783720 v^3 \\ & + 7143776640 v \cos(2v) + 55109134080 \sin(2v) + 45924278400 v \\ \Upsilon_6 & = 2041079040 \sin(v) v^2 - 26534027520 \cos(v) v - 55109134080 \sin(v) \\ \Upsilon_7 & = 2347 (\cos(v))^2 v^9 + 37552 \sin(v) \cos(v) v^8 \\ & + 4694 v^9 + 4040680 \sin(v) \cos(v) v^6 + 695352 \sin(v) v^6 \\ & + 11178636 (\cos(v))^2 v^5 + 166957 (\cos(v))^2 v^7 \\ & + 1007503 v^7 + 195817944 \sin(v) \cos(v) v^4 \\ & - 11820984 \cos(v) v^5 - 191111592 \sin(v) v^4 \\ & + 529550952 (\cos(v))^2 v^3 + 65816772 v^5 \\ & + 2737592928 \cos(v) v^3 + 13181968800 \sin(v) v^2 \\ & + 11906294400 (\cos(v))^2 v + 3827023200 \sin(v) \cos(v) v^2 \\ & + 701620920 v^3 + 23812588800 \sin(v) \cos(v) \\ & - 13607193600 \cos(v) v - 22111689600 v \\ \Upsilon_8 & = \sin(v) v^2 - 13 \cos(v) v - 27 \sin(v) \end{aligned}$$

$$\begin{aligned}
 \Upsilon_9 &= 2347 \sin(v) v^8 - 16429 \cos(v) v^7 \\
 &+ 190267 \sin(v) v^6 - 173838 \cos(v) v^5 \\
 &+ 10042326 \sin(v) v^4 + 40998216 \cos(v) v^3 \\
 &+ 106306200 \sin(v) v^2 - 5562816 v^3 \\
 &+ 1275674400 \cos(v) v - 2976573600 \sin(v) + 1700899200 v \\
 \Upsilon_{10} &= 2347 (\cos(v))^2 v^8 + 28164 \sin(v) \cos(v) v^7 \\
 &+ 4694 v^8 + 3161622 \sin(v) \cos(v) v^5 + 1390704 \sin(v) v^5 \\
 &+ 26476380 (\cos(v))^2 v^4 + 298389 (\cos(v))^2 v^6 \\
 &+ 927705 v^6 + 147626640 \sin(v) \cos(v) v^3 \\
 &- 20860560 \cos(v) v^4 - 275194080 \sin(v) v^3 \\
 &+ 1254413160 (\cos(v))^2 v^2 + 58167900 v^4 \\
 &+ 3614410800 \cos(v) v^2 + 13394581200 \sin(v) v \\
 &+ 21431329920 (\cos(v))^2 + 2678916240 \sin(v) \cos(v) v \\
 &+ 489008520 v^2 - 21431329920.
 \end{aligned}$$

Appendix C: Truncated Taylor Series Expansion Formulae for the coefficients of the newly introduced scheme given by (26)

$$\begin{aligned}
 a_1 &= -2 + \frac{53 v^{16}}{32330691993600} + \frac{110947 v^{18}}{762949533265920000} + \dots \\
 c_0 &= -\frac{592847}{422460} + \frac{53 v^6}{27882360}
 \end{aligned}$$

$$\begin{aligned}
 & - \frac{19682309 v^8}{15336537216000} - \frac{219307579 v^{10}}{1229319311220000} \\
 & - \frac{3640112453 v^{12}}{101155417608960000} - \frac{4233019325867 v^{14}}{584626439206656000000} \\
 & - \frac{66085951486477057 v^{16}}{45144853635537976320000000} \\
 & - \frac{722098054883861671 v^{18}}{2437822096319050721280000000} + \dots \\
 c_1 = & \frac{6253}{844920} + \frac{53 v^6}{55764720} + \frac{22944073 v^8}{92019223296000} \\
 & + \frac{380642117 v^{10}}{7152403265280000} + \frac{30861741653 v^{12}}{2832351693050880000} \\
 & + \frac{16802851104727 v^{14}}{7600143709686528000000} \\
 & + \frac{80846754137521861 v^{16}}{180579414542151905280000000} \\
 & + \frac{441848899882833299 v^{18}}{4875644192638101442560000000} + \dots \\
 c_2 = & \frac{92605}{86919} + \frac{53 v^{10}}{4130390880} + \frac{3275171 v^{12}}{2044708701235200} \\
 & + \frac{604517171 v^{14}}{1882704857983488000} + \frac{13506103459 v^{16}}{209787112746731520000} \\
 & + \frac{6590061176239 v^{18}}{506635877283356620800000} + \dots
 \end{aligned}$$

Appendix D: Expressions for the Derivatives of ε_n

Expressions of the derivatives which are presented in the formulae of the Local Truncation Errors:

$$\begin{aligned}
 \varepsilon^{(2)} &= (V(x) - V_c + \Gamma) \varepsilon(x) = (\Xi(x) + \Gamma) \varepsilon(x) \\
 \varepsilon^{(3)} &= \left(\frac{d}{dx} \Xi(x) \right) \varepsilon(x) + (\Xi(x) + \Gamma) \frac{d}{dx} \varepsilon(x)
 \end{aligned}$$

$$\begin{aligned}
 \varepsilon^{(4)} &= \left(\frac{d^2}{dx^2} \Xi(x) \right) \varepsilon(x) + 2 \left(\frac{d}{dx} \Xi(x) \right) \frac{d}{dx} \varepsilon(x) + (\Xi(x) + \Gamma)^2 \varepsilon(x) \\
 \varepsilon^{(5)} &= \left(\frac{d^3}{dx^3} \Xi(x) \right) \varepsilon(x) + 3 \left(\frac{d^2}{dx^2} \Xi(x) \right) \frac{d}{dx} \varepsilon(x) \\
 &+ 4 (\Xi(x) + \Gamma) \varepsilon(x) \frac{d}{dx} \Xi(x) + (\Xi(x) + \Gamma)^2 \frac{d}{dx} \varepsilon(x) \\
 \varepsilon^{(6)} &= \left(\frac{d^4}{dx^4} \Xi(x) \right) \varepsilon(x) + 4 \left(\frac{d^3}{dx^3} \Xi(x) \right) \frac{d}{dx} \varepsilon(x) \\
 &+ 7 (\Xi(x) + \Gamma) \varepsilon(x) \frac{d^2}{dx^2} \Xi(x) + 4 \left(\frac{d}{dx} \Xi(x) \right)^2 \varepsilon(x) \\
 &+ 6 (\Xi(x) + \Gamma) \left(\frac{d}{dx} \varepsilon(x) \right) \frac{d}{dx} \Xi(x) + (\Xi(x) + \Gamma)^3 \varepsilon(x) \\
 \varepsilon^{(7)} &= \left(\frac{d^5}{dx^5} \Xi(x) \right) \varepsilon(x) + 5 \left(\frac{d^4}{dx^4} \Xi(x) \right) \frac{d}{dx} \varepsilon(x) \\
 &+ 11 (\Xi(x) + \Gamma) \varepsilon(x) \frac{d^3}{dx^3} \Xi(x) + 15 \left(\frac{d}{dx} \Xi(x) \right) \varepsilon(x) \\
 &+ \frac{d^2}{dx^2} \Xi(x) + 13 (\Xi(x) + \Gamma) \left(\frac{d}{dx} \varepsilon(x) \right) \frac{d^2}{dx^2} \Xi(x) \\
 &+ 10 \left(\frac{d}{dx} \Xi(x) \right)^2 \frac{d}{dx} \varepsilon(x) + 9 (\Xi(x) + \Gamma)^2 \varepsilon(x) \\
 &+ \frac{d}{dx} \Xi(x) + (\Xi(x) + \Gamma)^3 \frac{d}{dx} \varepsilon(x) \\
 \varepsilon^{(8)} &= \left(\frac{d^6}{dx^6} \Xi(x) \right) \varepsilon(x) + 6 \left(\frac{d^5}{dx^5} \Xi(x) \right) \frac{d}{dx} \varepsilon(x) \\
 &+ 16 (\Xi(x) + \Gamma) \varepsilon(x) \frac{d^4}{dx^4} \Xi(x) + 26 \left(\frac{d}{dx} \Xi(x) \right) \varepsilon(x) \\
 &+ \frac{d^3}{dx^3} \Xi(x) + 24 (\Xi(x) + \Gamma) \left(\frac{d}{dx} \varepsilon(x) \right) \frac{d^3}{dx^3} \Xi(x) \\
 &+ 15 \left(\frac{d^2}{dx^2} \Xi(x) \right)^2 \varepsilon(x) + 48 \left(\frac{d}{dx} \Xi(x) \right)
 \end{aligned}$$

$$\begin{aligned}
 & + \left(\frac{d}{dx} \varepsilon(x) \right) \frac{d^2}{dx^2} \Xi(x) + 22 (\Xi(x) + \Gamma)^2 \varepsilon(x) \\
 & + \frac{d^2}{dx^2} \Xi(x) + 28 (\Xi(x) + \Gamma) \varepsilon(x) \left(\frac{d}{dx} \Xi(x) \right)^2 \\
 & + 12 (\Xi(x) + \Gamma)^2 \left(\frac{d}{dx} \varepsilon(x) \right) \frac{d}{dx} \Xi(x) + (\Xi(x) + \Gamma)^4 \varepsilon(x) \\
 & \dots
 \end{aligned}$$

We compute the j -th derivative of the function ε at the point x_n , i.e. $\varepsilon_n^{(j)}$, substituting in the above formulae x with x_n .

Appendix E: Formula for the quantity ζ_0

$$\begin{aligned}
 \zeta_0 = & \frac{53 \left(\frac{d^4}{dx^4} \Xi(x) \right) \varepsilon(x) \frac{d^8}{dx^8} \Xi(x)}{8074598400} + \frac{689 \left(\frac{d^3}{dx^3} \Xi(x) \right) \varepsilon(x) \frac{d^9}{dx^9} \Xi(x)}{177641164800} \\
 & + \frac{270883 \Xi(x) \varepsilon(x) \left(\frac{d}{dx} \Xi(x) \right)^2 \left(\frac{d^2}{dx^2} \Xi(x) \right)^2}{367394227200} \\
 & + \frac{26129 \Xi(x) \left(\frac{d}{dx} \varepsilon(x) \right) \left(\frac{d^6}{dx^6} \Xi(x) \right) \frac{d^3}{dx^3} \Xi(x)}{144333446400} \\
 & + \frac{371 \left(\frac{d^3}{dx^3} \Xi(x) \right) \left(\frac{d}{dx} \varepsilon(x) \right) \frac{d^8}{dx^8} \Xi(x)}{14803430400} \\
 & + \frac{11183 \left(\frac{d^2}{dx^2} \Xi(x) \right) \left(\frac{d}{dx} \varepsilon(x) \right) \left(\frac{d^3}{dx^3} \Xi(x) \right) \frac{d^4}{dx^4} \Xi(x)}{11102572800} \\
 & + \frac{5353 (\Xi(x))^2 \left(\frac{d}{dx} \varepsilon(x) \right) \left(\frac{d}{dx} \Xi(x) \right) \frac{d^6}{dx^6} \Xi(x)}{64148198400} \\
 & + \frac{53 (\Xi(x))^2 \left(\frac{d}{dx} \varepsilon(x) \right) \left(\frac{d^3}{dx^3} \Xi(x) \right) \frac{d^4}{dx^4} \Xi(x)}{198806400} \\
 & + \frac{87821 (\Xi(x))^2 \varepsilon(x) \left(\frac{d}{dx} \Xi(x) \right) \frac{d^7}{dx^7} \Xi(x)}{1347112166400}
 \end{aligned}$$

$$\begin{aligned}
 & + \frac{23797 \Xi(x) \left(\frac{d}{dx} \varepsilon(x)\right) \left(\frac{d^8}{dx^8} \Xi(x)\right) \frac{d}{dx} \Xi(x)}{673556083200} \\
 & + \frac{29839 \left(\frac{d^2}{dx^2} \Xi(x)\right) \varepsilon(x) \left(\frac{d^3}{dx^3} \Xi(x)\right) \frac{d^5}{dx^5} \Xi(x)}{88820582400} \\
 & + \frac{148771 \Xi(x) \left(\frac{d}{dx} \varepsilon(x)\right) \left(\frac{d}{dx} \Xi(x)\right) \left(\frac{d^4}{dx^4} \Xi(x)\right) \frac{d^2}{dx^2} \Xi(x)}{144333446400} \\
 & + \frac{26977 \left(\frac{d}{dx} \Xi(x)\right)^2 \left(\frac{d}{dx} \varepsilon(x)\right) \frac{d^7}{dx^7} \Xi(x)}{367394227200} \\
 & + \frac{371 \left(\frac{d^3}{dx^3} \Xi(x)\right)^3 \frac{d}{dx} \varepsilon(x)}{1850428800} + \frac{2809 (\Xi(x))^3 \left(\frac{d}{dx} \varepsilon(x)\right) \left(\frac{d^2}{dx^2} \Xi(x)\right) \frac{d^3}{dx^3} \Xi(x)}{28866689280} \\
 & + \frac{53 \left(\frac{d^2}{dx^2} \Xi(x)\right) \varepsilon(x) \frac{d^{10}}{dx^{10}} \Xi(x)}{29606860800} + \frac{53 \left(\frac{d^5}{dx^5} \Xi(x)\right) \left(\frac{d}{dx} \varepsilon(x)\right) \frac{d^6}{dx^6} \Xi(x)}{1009324800} \\
 & + \frac{53 \left(\frac{d^4}{dx^4} \Xi(x)\right) \left(\frac{d}{dx} \varepsilon(x)\right) \frac{d^7}{dx^7} \Xi(x)}{1284595200} + \frac{53 \left(\frac{d}{dx} \Xi(x)\right) \varepsilon(x) \frac{d^{11}}{dx^{11}} \Xi(x)}{85530931200} \\
 & + \frac{4823 \left(\frac{d^3}{dx^3} \Xi(x)\right)^2 \varepsilon(x) \frac{d^4}{dx^4} \Xi(x)}{22205145600} + \frac{1007 \left(\frac{d^5}{dx^5} \Xi(x)\right) \varepsilon(x) \frac{d^7}{dx^7} \Xi(x)}{113044377600} \\
 & + \frac{7897 \left(\frac{d}{dx} \Xi(x)\right)^3 \varepsilon(x) \frac{d^5}{dx^5} \Xi(x)}{52484889600} + \frac{624181 (\Xi(x))^2 \varepsilon(x) \left(\frac{d^4}{dx^4} \Xi(x)\right)^2}{4041336499200} \\
 & + \frac{39167 \left(\frac{d}{dx} \Xi(x)\right)^4 \varepsilon(x) \frac{d^2}{dx^2} \Xi(x)}{288666892800} + \frac{522739 \left(\frac{d}{dx} \Xi(x)\right)^2 \varepsilon(x) \left(\frac{d^3}{dx^3} \Xi(x)\right)^2}{1154667571200} \\
 & + \frac{8533 \left(\frac{d^2}{dx^2} \Xi(x)\right) \varepsilon(x) \left(\frac{d^4}{dx^4} \Xi(x)\right)^2}{44410291200} \\
 & + \frac{14893 (\Xi(x))^2 \left(\frac{d}{dx} \varepsilon(x)\right) \left(\frac{d}{dx} \Xi(x)\right) \left(\frac{d^2}{dx^2} \Xi(x)\right)^2}{52484889600} \\
 & + \frac{176543 (\Xi(x))^2 \varepsilon(x) \left(\frac{d^3}{dx^3} \Xi(x)\right) \frac{d^5}{dx^5} \Xi(x)}{673556083200}
 \end{aligned}$$

$$\begin{aligned}
 & + \frac{298867 (\Xi(x))^2 \varepsilon(x) \left(\frac{d}{dx}\Xi(x)\right) \left(\frac{d^3}{dx^3}\Xi(x)\right) \frac{d^2}{dx^2}\Xi(x)}{310872038400} \\
 & + \frac{53 \left(\frac{d}{dx}\Xi(x)\right) \left(\frac{d}{dx}\varepsilon(x)\right) \left(\frac{d^4}{dx^4}\Xi(x)\right)^2}{159045120} + \frac{371 (\Xi(x))^5 \left(\frac{d}{dx}\varepsilon(x)\right) \frac{d^3}{dx^3}\Xi(x)}{288666892800} \\
 & + \frac{53 (\Xi(x))^6 \varepsilon(x) \frac{d^2}{dx^2}\Xi(x)}{128296396800} + \frac{54007 \Xi(x) \varepsilon(x) \left(\frac{d^5}{dx^5}\Xi(x)\right)^2}{734788454400} \\
 & + \frac{1641569 (\Xi(x))^2 \varepsilon(x) \left(\frac{d^2}{dx^2}\Xi(x)\right)^3}{8082672998400} + \frac{371 \left(\frac{d}{dx}\Xi(x)\right) \left(\frac{d}{dx}\varepsilon(x)\right) \frac{d^{10}}{dx^{10}}\Xi(x)}{104969779200} \\
 & + \frac{438787 \left(\frac{d}{dx}\Xi(x)\right)^2 \varepsilon(x) \left(\frac{d^4}{dx^4}\Xi(x)\right) \frac{d^2}{dx^2}\Xi(x)}{577333785600} \\
 & + \frac{53 \left(\frac{d^{14}}{dx^{14}}\Xi(x)\right) \varepsilon(x)}{32330691993600} + \frac{53 \left(\frac{d^{13}}{dx^{13}}\Xi(x)\right) \frac{d}{dx}\varepsilon(x)}{2309335142400} \\
 & + \frac{53 \left(\frac{d^2}{dx^2}\Xi(x)\right)^4 \varepsilon(x)}{526344192} + \frac{33443 (\Xi(x))^3 \varepsilon(x) \left(\frac{d}{dx}\Xi(x)\right)^2 \frac{d^2}{dx^2}\Xi(x)}{288666892800} \\
 & + \frac{20087 \Xi(x) \left(\frac{d}{dx}\varepsilon(x)\right) \left(\frac{d}{dx}\Xi(x)\right)^3 \frac{d^2}{dx^2}\Xi(x)}{72166723200} + \frac{1007 (\Xi(x))^5 \varepsilon(x) \left(\frac{d}{dx}\Xi(x)\right)^2}{577333785600} \\
 & + \frac{53 \left(\frac{d}{dx}\Xi(x)\right) \left(\frac{d}{dx}\varepsilon(x)\right) \left(\frac{d^2}{dx^2}\Xi(x)\right)^3}{106913664} + \frac{1007 \left(\frac{d^2}{dx^2}\Xi(x)\right) \left(\frac{d}{dx}\varepsilon(x)\right) \frac{d^9}{dx^9}\Xi(x)}{88820582400} \\
 & + \frac{61427 \Xi(x) \varepsilon(x) \left(\frac{d}{dx}\Xi(x)\right)^2 \frac{d^6}{dx^6}\Xi(x)}{310872038400} + \frac{2173 (\Xi(x))^2 \varepsilon(x) \left(\frac{d}{dx}\Xi(x)\right)^4}{57733378560} \\
 & + \frac{169441 \left(\frac{d}{dx}\Xi(x)\right)^2 \left(\frac{d}{dx}\varepsilon(x)\right) \left(\frac{d^3}{dx^3}\Xi(x)\right) \frac{d^2}{dx^2}\Xi(x)}{144333446400} \\
 & + \frac{793781 \Xi(x) \varepsilon(x) \left(\frac{d}{dx}\Xi(x)\right)^3 \frac{d^3}{dx^3}\Xi(x)}{2020668249600} \\
 & + \frac{25387 \left(\frac{d}{dx}\Xi(x)\right) \varepsilon(x) \left(\frac{d^6}{dx^6}\Xi(x)\right) \frac{d^3}{dx^3}\Xi(x)}{128296396800}
 \end{aligned}$$

$$\begin{aligned}
 & + \frac{232511 \Xi(x) \left(\frac{d}{dx} \varepsilon(x)\right) \left(\frac{d^2}{dx^2} \Xi(x)\right)^2 \frac{d^3}{dx^3} \Xi(x)}{288666892800} \\
 & + \frac{2334809 \Xi(x) \varepsilon(x) \left(\frac{d^3}{dx^3} \Xi(x)\right) \left(\frac{d^4}{dx^4} \Xi(x)\right) \frac{d}{dx} \Xi(x)}{2020668249600} \\
 & + \frac{63017 (\Xi(x))^2 \left(\frac{d}{dx} \varepsilon(x)\right) \left(\frac{d}{dx} \Xi(x)\right)^2 \frac{d^3}{dx^3} \Xi(x)}{288666892800} \\
 & + \frac{53 (\Xi(x))^6 \left(\frac{d}{dx} \varepsilon(x)\right) \frac{d}{dx} \Xi(x)}{577333785600} + \frac{2491 \left(\frac{d}{dx} \Xi(x)\right)^2 \varepsilon(x) \frac{d^8}{dx^8} \Xi(x)}{104969779200} \\
 & + \frac{53 \left(\frac{d^6}{dx^6} \Xi(x)\right)^2 \varepsilon(x)}{10766131200} + \frac{2491 \left(\frac{d}{dx} \Xi(x)\right) \varepsilon(x) \left(\frac{d^5}{dx^5} \Xi(x)\right) \frac{d^4}{dx^4} \Xi(x)}{9542707200} \\
 & + \frac{65243 \Xi(x) \varepsilon(x) \left(\frac{d^2}{dx^2} \Xi(x)\right)^2 \frac{d^4}{dx^4} \Xi(x)}{91848556800} + \frac{2491 \Xi(x) \varepsilon(x) \left(\frac{d^9}{dx^9} \Xi(x)\right) \frac{d}{dx} \Xi(x)}{168389020800} \\
 & + \frac{265 \left(\frac{d}{dx} \Xi(x)\right)^3 \left(\frac{d}{dx} \varepsilon(x)\right) \frac{d^4}{dx^4} \Xi(x)}{1049697792} \\
 & + \frac{3551 \left(\frac{d^2}{dx^2} \Xi(x)\right)^2 \left(\frac{d}{dx} \varepsilon(x)\right) \frac{d^5}{dx^5} \Xi(x)}{9868953600} \\
 & + \frac{12137 \left(\frac{d}{dx} \Xi(x)\right) \varepsilon(x) \left(\frac{d^7}{dx^7} \Xi(x)\right) \frac{d^2}{dx^2} \Xi(x)}{107768973312} + \frac{1219 \Xi(x) \varepsilon(x) \left(\frac{d^{12}}{dx^{12}} \Xi(x)\right)}{8082672998400} \\
 & + \frac{583 \Xi(x) \left(\frac{d}{dx} \varepsilon(x)\right) \left(\frac{d^5}{dx^5} \Xi(x)\right) \frac{d^4}{dx^4} \Xi(x)}{2385676800} \\
 & + \frac{31747 (\Xi(x))^3 \varepsilon(x) \left(\frac{d^2}{dx^2} \Xi(x)\right) \frac{d^4}{dx^4} \Xi(x)}{202066824960} \\
 & + \frac{168169 (\Xi(x))^3 \varepsilon(x) \left(\frac{d}{dx} \Xi(x)\right) \frac{d^5}{dx^5} \Xi(x)}{2020668249600} \\
 & + \frac{8851 \Xi(x) \left(\frac{d}{dx} \varepsilon(x)\right) \left(\frac{d}{dx} \Xi(x)\right)^2 \frac{d^5}{dx^5} \Xi(x)}{32074099200} \\
 & + \frac{65773 \Xi(x) \varepsilon(x) \left(\frac{d}{dx} \Xi(x)\right) \left(\frac{d^5}{dx^5} \Xi(x)\right) \frac{d^2}{dx^2} \Xi(x)}{80826729984}
 \end{aligned}$$

$$\begin{aligned} & + \frac{164353 \left(\frac{d}{dx} \Xi(x) \right) \left(\frac{d}{dx} \varepsilon(x) \right) \left(\frac{d^5}{dx^5} \Xi(x) \right) \frac{d^3}{dx^3} \Xi(x)}{288666892800} \\ & + \frac{5671 \Xi(x) \left(\frac{d}{dx} \varepsilon(x) \right) \left(\frac{d^3}{dx^3} \Xi(x) \right)^2 \frac{d}{dx} \Xi(x)}{9020840400} \\ & + \frac{35351 \left(\Xi(x) \right)^2 \left(\frac{d}{dx} \varepsilon(x) \right) \left(\frac{d^2}{dx^2} \Xi(x) \right) \frac{d^5}{dx^5} \Xi(x)}{192444595200} \\ & + \frac{11819 \Xi(x) \varepsilon(x) \left(\frac{d^6}{dx^6} \Xi(x) \right) \frac{d^4}{dx^4} \Xi(x)}{91848556800} \\ & + \frac{371 \left(\Xi(x) \right)^3 \left(\frac{d}{dx} \varepsilon(x) \right) \left(\frac{d}{dx} \Xi(x) \right)^3}{28866689280} \\ & + \frac{265 \left(\frac{d^2}{dx^2} \Xi(x) \right)^2 \varepsilon(x) \frac{d^6}{dx^6} \Xi(x)}{2368548864} \\ & + \frac{4717 \left(\Xi(x) \right)^2 \varepsilon(x) \frac{d^{10}}{dx^{10}} \Xi(x)}{2694224332800} + \frac{53 \left(\Xi(x) \right)^5 \varepsilon(x) \frac{d^4}{dx^4} \Xi(x)}{18041680800} \\ & + \frac{67363 \left(\frac{d}{dx} \Xi(x) \right) \left(\frac{d}{dx} \varepsilon(x) \right) \left(\frac{d^6}{dx^6} \Xi(x) \right) \frac{d^2}{dx^2} \Xi(x)}{192444595200} \\ & + \frac{170713 \Xi(x) \varepsilon(x) \left(\frac{d^8}{dx^8} \Xi(x) \right) \frac{d^2}{dx^2} \Xi(x)}{4041336499200} \\ & + \frac{346037 \Xi(x) \varepsilon(x) \left(\frac{d^7}{dx^7} \Xi(x) \right) \frac{d^3}{dx^3} \Xi(x)}{4041336499200} \\ & + \frac{97997 \Xi(x) \left(\frac{d}{dx} \varepsilon(x) \right) \left(\frac{d^7}{dx^7} \Xi(x) \right) \frac{d^2}{dx^2} \Xi(x)}{1010334124800} \\ & + \frac{16271 \left(\frac{d}{dx} \Xi(x) \right) \varepsilon(x) \left(\frac{d^2}{dx^2} \Xi(x) \right)^2 \frac{d^3}{dx^3} \Xi(x)}{15395567616} \\ & + \frac{6307 \Xi(x) \varepsilon(x) \left(\frac{d^2}{dx^2} \Xi(x) \right) \left(\frac{d^3}{dx^3} \Xi(x) \right)^2}{7401715200} \end{aligned}$$

$$\begin{aligned}
 & + \frac{110399 (\Xi(x))^4 \varepsilon(x) \frac{d^6}{dx^6} \Xi(x)}{16165345996800} + \frac{48707 (\Xi(x))^3 \varepsilon(x) \left(\frac{d^3}{dx^3} \Xi(x) \right)^2}{505167062400} \\
 & + \frac{16589 (\Xi(x))^4 \varepsilon(x) \left(\frac{d^2}{dx^2} \Xi(x) \right)^2}{769778380800} + \frac{1643 (\Xi(x))^2 \left(\frac{d}{dx} \varepsilon(x) \right) \frac{d^9}{dx^9} \Xi(x)}{449037388800} \\
 & + \frac{2173 (\Xi(x))^3 \left(\frac{d}{dx} \varepsilon(x) \right) \left(\frac{d}{dx} \Xi(x) \right) \frac{d^4}{dx^4} \Xi(x)}{36083361600} \\
 & + \frac{371 (\Xi(x))^4 \left(\frac{d}{dx} \varepsilon(x) \right) \left(\frac{d}{dx} \Xi(x) \right) \frac{d^2}{dx^2} \Xi(x)}{28866689280} \\
 & + \frac{38213 (\Xi(x))^4 \varepsilon(x) \left(\frac{d}{dx} \Xi(x) \right) \frac{d^3}{dx^3} \Xi(x)}{1154667571200} + \frac{53 \left(\frac{d}{dx} \Xi(x) \right)^5 \frac{d}{dx} \varepsilon(x)}{2624244480} \\
 & + \frac{53 (\Xi(x))^8 \varepsilon(x)}{32330691993600} + \frac{1277989 (\Xi(x))^2 \varepsilon(x) \left(\frac{d^2}{dx^2} \Xi(x) \right) \frac{d^6}{dx^6} \Xi(x)}{8082672998400} \\
 & + \frac{23479 (\Xi(x))^3 \varepsilon(x) \frac{d^8}{dx^8} \Xi(x)}{4041336499200} + \frac{901 (\Xi(x))^3 \left(\frac{d}{dx} \varepsilon(x) \right) \frac{d^7}{dx^7} \Xi(x)}{126291765600} \\
 & + \frac{1961 (\Xi(x))^4 \left(\frac{d}{dx} \varepsilon(x) \right) \frac{d^5}{dx^5} \Xi(x)}{384889190400} + \frac{2491 \Xi(x) \left(\frac{d}{dx} \varepsilon(x) \right) \frac{d^{11}}{dx^{11}} \Xi(x)}{4041336499200} \\
 & + \frac{622697 (\Xi(x))^2 \varepsilon(x) \left(\frac{d}{dx} \Xi(x) \right)^2 \frac{d^4}{dx^4} \Xi(x)}{2020668249600}
 \end{aligned}$$

at every point $x = x_n$.

Appendix F: Formulae for the $\Upsilon_j(v)$, $j = 11(1)13$

$$\begin{aligned}
 \Upsilon_{11}(s, v) &= -2347 \sin(v) s^8 v^8 + 2347 \sin(v) s^6 v^{10} \\
 &- 30511 \cos(v) s^6 v^9 - 190267 \sin(v) s^8 v^6 \\
 &- 63369 \sin(v) s^6 v^8 + 173838 \sin(v) s^4 v^{10} \\
 &+ 173838 \cos(v) s^8 v^5 - 2259894 \cos(v) s^4 v^9 \\
 &- 10042326 \sin(v) s^8 v^4 - 4693626 \sin(v) s^4 v^8
 \end{aligned}$$

$$\begin{aligned} &+ 7087080 \sin(v) s^2 v^{10} - 40998216 \cos(v) s^8 v^3 \\ &- 92132040 \cos(v) s^2 v^9 - 106306200 \sin(v) s^8 v^2 \\ &- 191351160 \sin(v) s^2 v^8 + 85044960 \sin(v) v^{10} \\ &+ 5562816 s^8 v^3 - 1275674400 \cos(v) s^8 v \\ &- 1105584480 \cos(v) v^9 + 2976573600 \sin(v) s^8 \\ &- 2296213920 \sin(v) v^8 - 1700899200 s^8 v \\ &+ 16429 \cos(v) s^8 v^7 \end{aligned}$$

$$\Upsilon_{12}(s, v) = v^8 (-\sin(v) v^2 + 13 \cos(v) v + 27 \sin(v))$$

$$\begin{aligned} \Upsilon_{13}(s, v) &= -180520200 \sin(v) \cos(v) v^{12} - 573334776 \sin(v) s^8 v^4 \\ &- 14457643200 \cos(v) s^6 v^5 - 1193556 (\cos(v))^2 s^6 v^9 \\ &+ 33535908 (\cos(v))^2 s^8 v^5 - 5562816 \sin(v) s^6 v^8 \\ &- 850449600 \sin(v) s^2 v^{10} - 105905520 (\cos(v))^2 s^6 v^7 \\ &+ 39545906400 \sin(v) s^8 v^2 + 500871 (\cos(v))^2 s^8 v^7 \\ &- 55109134080 \sin(v) \cos(v) v^8 - 112647024 \sin(v) s^4 v^8 \\ &- 1390704 \sin(v) \cos(v) v^{14} + 83442240 \cos(v) s^6 v^7 \\ &+ 4172112 \sin(v) s^4 v^{10} - 85725319680 (\cos(v))^2 s^6 v^3 \\ &- 9388 (\cos(v))^2 s^6 v^{11} + 11055844800 \cos(v) s^2 v^9 \\ &+ 7041 (\cos(v))^2 s^8 v^9 + 2086056 \sin(v) s^8 v^6 \end{aligned}$$

$$\begin{aligned} & - 54237456 \cos(v) s^4 v^9 - 5868102240 \sin(v) \cos(v) v^{10} \\ & + 22962139200 \sin(v) s^2 v^8 - 40821580800 \cos(v) s^8 v \\ & + 71437766400 \sin(v) \cos(v) s^8 - 35462952 \cos(v) s^8 v^5 \\ & + 35718883200 (\cos(v))^2 s^8 v - 5017652640 (\cos(v))^2 s^6 v^5 \\ & + 8212778784 \cos(v) s^8 v^3 + 35221284 v^{13} - 148828680 v^{11} \\ & - 695352 \sin(v) v^{14} + 1100776320 \sin(v) s^6 v^6 \\ & + 6258168 \cos(v) v^{13} + 435655080 \sin(v) v^{12} \\ & - 4677472800 \cos(v) v^{11} - 232671600 s^6 v^7 \\ & + 85725319680 s^6 v^3 - 18776 s^6 v^{11} + 4694 v^{17} \\ & + 688311 v^{15} - 19390250880 v^9 \\ & + 3022509 s^8 v^7 - 3710820 s^6 v^9 \\ & + 197450316 s^8 v^5 - 1956034080 s^6 v^5 \\ & - 7143776640 (\cos(v))^2 v^9 + 2104862760 s^8 v^3 \\ & - 8929720800 \sin(v) v^{10} + 14082 s^8 v^9 + 2347 (\cos(v))^2 v^{17} \\ & + 354717 (\cos(v))^2 v^{15} - 66335068800 s^8 v \\ & + 22304268 (\cos(v))^2 v^{13} + 233873640 (\cos(v))^2 v^{11} \\ & - 112656 \sin(v) \cos(v) s^6 v^{10} + 12122040 \sin(v) \cos(v) s^8 v^6 \\ & - 12646488 \sin(v) \cos(v) s^6 v^8 + 112656 \sin(v) \cos(v) s^8 v^8 \end{aligned}$$

$$\begin{aligned} &+ 587453832 \sin(v) \cos(v) s^8 v^4 - 590506560 \sin(v) \cos(v) s^6 v^6 \\ &- 10715664960 \sin(v) \cos(v) s^6 v^4 + 1588652856 (\cos(v))^2 s^8 v^3 \\ &+ 11481069600 \sin(v) \cos(v) s^8 v^2 - 53578324800 \sin(v) s^6 v^4. \end{aligned}$$

References

- [1] F. Hui, T. E. Simos, Hybrid high algebraic order two-step method with vanished phase-lag and its first and second derivatives, *MATCH Commun. Math. Comput. Chem.* **73** (2015) 619–648.
- [2] J. Ma, T. E. Simos, Runge–Kutta type tenth algebraic order two-step method with vanished phase-lag and its first, second and third derivatives, *MATCH Commun. Math. Comput. Chem.* **74** (2015) 609–644.
- [3] Z. Zhou, T. E. Simos, Three-stages tenth algebraic order two-step method with vanished phase-lag and its first, second, third and fourth derivatives, *MATCH Commun. Math. Comput. Chem.* **75** (2015) 653–694.
- [4] T. Lei, T. E. Simos, Four-stages twelfth algebraic order two-step method with vanished phase-lag and its first and second derivatives, for the numerical solution of the Schrödinger equation *MATCH Commun. Math. Comput. Chem.* **76** (2016) 475–510.
- [5] T. Lei, T. E. Simos, A new four-stages high algebraic order two-step method with vanished phase-lag and its first, second and third derivatives for the numerical solution of the Schrödinger equation, *MATCH Commun. Math. Comput. Chem.* **77** (2017) 333–392.
- [6] M. A. Medvedev, T. E. Simos, New high order P-stable method with optimal phase properties, *MATCH Commun. Math. Comput. Chem.* **79** (2018) 175–214.
- [7] M. A. Medvedev, T. E. Simos, A new high order method with optimal stability and phase properties, *MATCH Commun. Math. Comput. Chem.* **79** (2018) 215–260.
- [8] M. A. Medvedev, T. E. Simos, A new high order finite difference pair with improved properties, *MATCH Commun. Math. Comput. Chem.* **80** (2018) 481–536.
- [9] V. N. Kovalnogov, R. V. Fedorov, A. A. Bondarenko, T. E. Simos, An optimized multistage complete in phase P-stable algorithm, *MATCH Commun. Math. Comput. Chem.* **82** (2019) 385–438.
- [10] R. Vujasin, M. Senčanski, J. Radić–Perić, M. Perić, A comparison of various variational approaches for solving the one-dimensional vibrational Schrödinger equation, *MATCH Commun. Math. Comput. Chem.* **63** (2010) 363–378.
- [11] C. J. Cramer, *Essentials of Computational Chemistry*, Wiley, Chichester, 2004.

- [12] F. Jensen, *Introduction to Computational Chemistry*, Wiley, Chichester, 2007.
- [13] A. R. Leach, *Molecular Modelling – Principles and Applications*, Pearson, Essex, 2001.
- [14] P. Atkins, R. Friedman, *Molecular Quantum Mechanics*, Oxford Univ. Press, Oxford, 2011.
- [15] Z. A. Anastassi, T. E. Simos, A parametric symmetric linear four–step method for the efficient integration of the Schrödinger equation and related oscillatory problems, *J. Comp. Appl. Math.* **236** (2012) 3880–3889.
- [16] J. D. Lambert, I. A. Watson, Symmetric multistep methods for periodic initial values problems, *J. Inst. Math. Appl.* **18** (1976) 189–202.
- [17] T. E. Simos, P. S. Williams, A finite–difference method for the numerical solution of the Schrödinger equation, *J. Comp. Appl. Math.* **79** (1997) 189–205.
- [18] R. M. Thomas, Phase properties of high order almost P -stable formulae, *BIT* **24** (1984) 225–238.
- [19] A. D. Raptis, T. E. Simos, A four–step phase–fitted method for the numerical integration of second order initial–value problem, *BIT* **31** (1991) 160–168.
- [20] L. G. Ixaru, M. Rizea, Comparison of some four–step methods for the numerical solution of the Schrödinger equation, *Comput. Phys. Commun.* **38** (1985) 329–337.
- [21] L. G. Ixaru, M. Micu, *Topics in Theoretical Physics*, Central Inst. Phys., Bucharest, 1978.
- [22] L. G. Ixaru, M. Rizea, A Numerov-like scheme for the numerical solution of the Schrödinger equation in the deep continuum spectrum of energies, *Comput. Phys. Commun.* **19** (1980) 23–27.
- [23] J. R. Dormand, M. E. A. El–Mikkawy, P. J. Prince, Families of Runge–Kutta–Nyström formulae, *IMA J. Numer. Anal.* **7** (1987) 235–250.
- [24] J. R. Dormand, P. J. Prince, A family of embedded Runge–Kutta formulae, *J. Comput. Appl. Math.* **6** (1980) 19–26.
- [25] G. D. Quinlan, S. Tremaine, Symmetric multistep methods for the numerical integration of planetary orbits, *Astronom. J.* **100** (1990) 1694–1700.
- [26] M. M. Chawla, P. S. Rao, An Noumerov–type method with minimal phase–lag for the integration of second order periodic initial–value problems. II. Explicit method, *J. Comput. Appl. Math.* **15** (1986) 329–337.
- [27] A. D. Raptis, A. C. Allison, Exponential–fitting methods for the numerical solution of the Schrödinger equation, *Comput. Phys. Commun.* **14** (1978) 1–5.
- [28] M. M. Chawla, P. S. Rao, An explicit sixth–order method with phase–lag of order eight for $y'' = f(t, y)$, *J. Comput. Appl. Math.* **17** (1987) 363–368.

- [29] T. E. Simos, On the explicit four-step methods with vanished phase-lag and its first derivative, *Appl. Math. Inf. Sci.* **8** (2014) 447–458.
- [30] A. C. Allison, The numerical solution of coupled differential equations arising from the Schrödinger equation, *J. Comput. Phys.* **6** (1970) 378–391.
- [31] R. B. Bernstein, A. Dalgarno, H. Massey, I. C. Percival, Thermal scattering of atoms by homonuclear diatomic molecules, *Proc. Roy. Soc. Ser. A* **274** (1963) 427–442.
- [32] R. B. Bernstein, Quantum mechanical (phase shift) analysis of differential elastic scattering of molecular beams, *J. Chem. Phys.* **33** (1960) 795–804.
- [33] A. D. Raptis, J. R. Cash, A variable step method for the numerical integration of the one-dimensional Schrödinger equation, *Comput. Phys. Commun.* **36** (1985) 113–119.
- [34] T. E. Simos, Exponentially fitted Runge–Kutta methods for the numerical solution of the Schrödinger equation and related problems, *Comput. Mater. Sci.* **18** (2000) 315–332.
- [35] G. A. Panopoulos, T. E. Simos, A new optimized symmetric embedded predictor–corrector method (EPCM) for initial–value problems with oscillatory solutions, *Appl. Math. Inf. Sci.* **8** (2014) 703–713.
- [36] J. M. Franco, M. Palacios, High-order P -stable multistep methods, *J. Comput. Appl. Math.* **30** (1990) 1–10.
- [37] J. D. Lambert, *Numerical Methods for Ordinary Differential Systems. The Initial Value Problem*, Wiley, New York, 1991, pp. 104–107.
- [38] E. Stiefel, D. G. Bettis, Stabilization of Cowell’s method, *Num. Math.* **13** (1969) 154–175.
- [39] G. A. Panopoulos, Z. A. Anastassi, T. E. Simos, Two new optimized eight-step symmetric methods for the efficient solution of the Schrödinger equation and related problems, *MATCH Commun. Math. Comput. Chem.* **60** (2008) 773–785.
- [40] T. E. Simos, G. Psihoyios, Preface, in: *Selected Papers of the International Conference on Computational Methods in Sciences and Engineering (ICCMSE 2003)*, *J. Comput. Appl. Math.* **175** (2005) IX–IX.
- [41] T. Lyche, Chebyshevian multistep methods for ordinary differential equations, *Numer. Math.* **19** (1972) 65–75.
- [42] A. Konguetsof, T. E. Simos, A generator of hybrid symmetric four-step methods for the numerical solution of the Schrödinger equation, *J. Comput. Appl. Math.* **158** (2003) 93–106.
- [43] Z. Kalogiratou, T. Monovasilis, T. E. Simos, Symplectic integrators for the numerical solution of the Schrödinger equation, *J. Comput. Appl. Math.* **158** (2003) 83–92.
- [44] Z. Kalogiratou, T. E. Simos, Newton–Cotes formulae for long-time integration, *J. Comput. Appl. Math.* **158** (2003) 75–82.

- [45] G. Psihoyios, T. E. Simos, Trigonometrically fitted predictor–corrector methods for IVPs with oscillating solutions, *J. Comput. Appl. Math.* **158** (2003) 135–144.
- [46] T. E. Simos, I. T. Famelis, C. Tsitouras, Zero dissipative, explicit Numerov–type methods for second order IVPs with oscillating solutions, *Numer. Algor.* **34** (2003) 27–40.
- [47] T. E. Simos, Dissipative trigonometrically–fitted methods for linear second-order IVPs with oscillating solution, *Appl. Math. Lett.* **17** (2004) 601–607.
- [48] K. Tselios, T. E. Simos, Runge–Kutta methods with minimal dispersion and dissipation for problems arising from computational acoustics, *J. Comput. Appl. Math.* **175** (2005) 173–181.
- [49] D. P. Sakas, T. E. Simos, Multiderivative methods of eighth algebraic order with minimal phase–lag for the numerical solution of the radial Schrödinger equation, *J. Comput. Appl. Math.* **175** (2005) 161–172.
- [50] G. Psihoyios, T. E. Simos, A fourth algebraic order trigonometrically fitted predictor–corrector scheme for IVPs with oscillating solutions, *J. Comput. Appl. Math.* **175** (2005) 137–147.
- [51] Z. A. Anastassi, T. E. Simos, An optimized Runge–Kutta method for the solution of orbital problems, *J. Comput. Appl. Math.* **175** (2005) 1–9.
- [52] T. E. Simos, Closed Newton–Cotes trigonometrically–fitted formulae of high order for long–time integration of orbital problems, *Appl. Math. Lett.* **22** (2009) 1616–1621.
- [53] S. Stavroyiannis, T. E. Simos, Optimization as a function of the phase–lag order of nonlinear explicit two–step P -stable method for linear periodic IVPs, *Appl. Numer. Math.* **59** (2009) 2467–2474.
- [54] T. E. Simos, Exponentially and trigonometrically fitted methods for the solution of the Schrödinger equation, *Acta Appl. Math.* **110** (2010) 1331–1352.
- [55] T. E. Simos, New stable closed Newton–Cotes trigonometrically fitted formulae for long–time integration, *Abstract Appl. Anal.* (2012) #182536.
- [56] T. E. Simos, Optimizing a hybrid two–step method for the numerical solution of the Schrödinger equation and related problems with respect to phase–lag, *J. Appl. Math.* (2012) #420387.
- [57] D. F. Papadopoulos, T. E. Simos, A modified Runge–Kutta–Nyström method by using phase lag properties for the numerical solution of orbital problems, *Appl. Math. Inf. Sci.* **7** (2013) 433–437.
- [58] T. Monovasilis, Z. Kalogiratou, T. E. Simos, Exponentially fitted symplectic Runge–Kutta–Nyström methods, *Appl. Math. Inf. Sci.* **7** (2013) 81–85.
- [59] G. A. Panopoulos, T. E. Simos, An optimized symmetric 8-step semi–embedded predictor–corrector method for IVPs with oscillating solutions, *Appl. Math. Inf. Sci.* **7** (2013) 73–80.

- [60] D. F. Papadopoulos, T. E. Simos, The use of phase lag and amplification error derivatives for the construction of a modified Runge–Kutta–Nyström method, *Abstract Appl. Anal.* (2013) #910624.
- [61] I. Alolyan, Z. A. Anastassi, T. E. Simos, A new family of symmetric linear four-step methods for the efficient integration of the Schrödinger equation and related oscillatory problems, *Appl. Math. Comput.* **218** (2012) 5370–5382.
- [62] I. Alolyan, T. E. Simos, A family of high-order multistep methods with vanished phase-lag and its derivatives for the numerical solution of the Schrödinger equation, *Comput. Math. Appl.* **62** (2011) 3756–3774.
- [63] C. Tsitouras, I. T. Famelis, T. E. Simos, On modified Runge–Kutta trees and methods, *Comput. Math. Appl.* **62** (2011) 2101–2111.
- [64] C. Tsitouras, I. T. Famelis, T. E. Simos, Phase-fitted Runge–Kutta pairs of orders 8(7), *J. Comp. Appl. Math.* **321** (2017) 226–231.
- [65] T. E. Simos, C. Tsitouras, Evolutionary generation of high order, explicit two step methods for second order linear IVPs, *Math. Methods Appl. Sci.* **40** (2017) 6276–6284.
- [66] A. A. Kosti, Z. A. Anastassi, T. E. Simos, Construction of an optimized explicit Runge–Kutta–Nyström method for the numerical solution of oscillatory initial value problems, *Comput. Math. Appl.* **61** (2011) 3381–3390.
- [67] Z. Kalogiratou, T. Monovasilis, T. E. Simos, New modified Runge–Kutta–Nyström methods for the numerical integration of the Schrödinger equation, *Comput. Math. Appl.* **60** (2010) 1639–1647.
- [68] T. Monovasilis, Z. Kalogiratou, T. E. Simos, A family of trigonometrically fitted partitioned Runge–Kutta symplectic methods, *Appl. Math. Comput.* **209** (2009) 91–96.
- [69] T. Monovasilis, Z. Kalogiratou, H. Ramos, T. E. Simos, Modified two-step hybrid methods for the numerical integration of oscillatory problems, *Math. Methods Appl. Sci.* **40** (2017) 5286–5292.
- [70] T. E. Simos, C. Tsitouras, I. T. Famelis, Explicit Numerov type methods with constant coefficients: A review, *Appl. Comput. Math.* **16** (2017) 89–113.
- [71] T. E. Simos, High order closed Newton–Cotes trigonometrically-fitted formulae for the numerical solution of the Schrödinger equation, *Appl. Math. Comput.* **209** (2009) 137–151.
- [72] T. E. Simos, Multistage symmetric two-step P-stable method with vanished phase-lag and its first, second and third derivatives, *Appl. Comput. Math.* **14** (2015) 296–315.
- [73] F. Hui, T. E. Simos, Four stages symmetric two-step P-stable method with vanished phase-lag and its first, second, third and fourth derivatives, *Appl. Comput. Math.* **15** (2016) 220–238

- [74] G. A. Panopoulos, T. E. Simos, An eight-step semi-embedded predictor-corrector method for orbital problems and related IVPs with oscillatory solutions for which the frequency is unknown, *J. Comp. Appl. Math.* **290** (2015) 1–15.
- [75] H. Ramos, Z. Kalogiratu, Th. Monovasilis, T. E. Simos, An optimized two-step hybrid block method for solving general second order initial-value problems, *Numerical Algorithms* **72** (2016) 1089–1102.
- [76] Z. Kalogiratu, T. Monovasilis, H. Ramos, T. E. Simos, A new approach on the construction of trigonometrically fitted two step hybrid methods, *J. Comp. Appl. Math.* **303** (2016) 146–155.
- [77] T. Monovasilis, Z. Kalogiratu, T. E. Simos, Construction of exponentially fitted symplectic Runge–Kutta–Nyström methods from partitioned Runge–Kutta methods, *Mediterr. J. Math.* **13** (2016) 2271–2285.
- [78] A. Konguetsof, T. E. Simos, An exponentially-fitted and trigonometrically-fitted method for the numerical solution of periodic initial-value problems, *Comput. Math. Appl.* **45** (2003) 547–554.
- [79] D. F. Papadopoulos, Z. A. Anastassi, T. E. Simos, An optimized Runge–Kutta–Nyström method for the numerical solution of the Schrödinger equation and related problems, *MATCH Commun. Math. Comput. Chem.* **64** (2010) 551–566.
- [80] Z. A. Anastassi, T. E. Simos, Trigonometrically fitted six-step symmetric methods for the efficient solution of the Schrödinger equation, *MATCH Commun. Math. Comput. Chem.* **60** (2008) 733–752.
- [81] W. Zhang, T. E. Simos, A high-order two-step phase-fitted method for the numerical solution of the Schrödinger equation, *Mediterr. J. Math.* **13** (2016) 5177–5194.
- [82] M. Dong, T. E. Simos, A new high algebraic order efficient finite difference method for the solution of the Schrödinger equation, *Filomat* **31** (2017) 4999–5012.
- [83] T. E. Simos, A new Numerov-type method for the numerical solution of the Schrödinger equation, *J. Math. Chem.* **46** (2009) 981–1007.
- [84] Z. Wang, P-stable linear symmetric multistep methods for periodic initial-value problems, *Comput. Phys. Commun.* **171** (2005) 162–174.
- [85] W. E. Boyce, R. D. DiPrima, *Elementary Differential Equations and Boundary Value Problems*, Wiley, New York, 1969.
- [86] T. E. Simos, C. Tsitouras, A new family of 7 stages, eighth-order explicit Numerov-type methods, *Math. Methods Appl. Sci.* **40** (2017) 7867–7878.
- [87] D. B. Berg, T. E. Simos, C. Tsitouras, Trigonometric fitted, eighth-order explicit Numerov-type methods, *Math. Methods Appl. Sci.* **41** (2018) 1845–1854.
- [88] T. E. Simos, C. Tsitouras, Fitted modifications of classical Runge–Kutta pairs of orders 5(4), *Math. Methods Appl. Sci.* **41** (2018) 4549–4559.
- [89] C. Tsitouras, T.E. Simos, On ninth order, explicit Numerov type methods with constant coefficients, *Mediterr. J. Math.* **15** (2018) #46.

- [90] M. A. Medvedev, T. E. Simos, C. Tsitouras, Fitted modifications of Runge–Kutta pairs of orders 6(5), *Math. Methods Appl. Sci.* **41** (2018) 6184–6194.
- [91] C. Tsitouras, T. E. Simos, Trigonometric fitted explicit Numerov type method with vanishing phase-lag and its first and second derivatives, *Mediterr. J. Math.* **15** (2018) #168.
- [92] M. A. Medvedev, T. E. Simos, C. Tsitouras, Explicit, two stage, sixth order, hybrid four–step methods for solving $y''(x) = f(x, y)$, *Math. Methods Appl. Sci.* **41** (2018) 6997–7006.
- [93] T. E. Simos, C. Tsitouras, High phase–lag order, four–step methods for solving $y'' = f(x, y)$, *Appl. Comput. Math.* **17** (2018) 307–316.
- [94] M. A. Medvedev, T. E. Simos, C. Tsitouras, Trigonometric–fitted hybrid four–step methods of sixth order for solving $y''(x) = f(x, y)$, *Math. Methods Appl. Sci.* **42** (2019) 710–716.
- [95] M. A. Medvedev, T. E. Simos, C. Tsitouras, Hybrid, phase-fitted, four-step methods of seventh order for solving $x''(t) = f(t, x)$, *Math. Methods Appl. Sci.* **42** (2019) 2025–2032.
- [96] J. Fang, C. Liu, C. W. Hsu, T. E. Simos, C. Tsitouras, Explicit hybrid six–step, sixth order, fully symmetric methods for solving $y''(x) = f(x, y)$, *Math. Methods Appl. Sci.* **42** (2019) 3305–3314.
- [97] C. Lin, J. J. Chen, T. E. Simos, C. Tsitouras, Evolutionary derivation of sixth-order P-stable SDIRKN methods for the solution of PDEs with the method of lines, *Mediterr. J. Math.* **16** (2019) #69.
- [98] N. Kovalnogov, E. Nadyseva, O. Shakhov, V. Kovalnogov, Control of turbulent transfer in the boundary layer through applied periodic effects, *Izvestiya Vysshikh Uchebnykh Zavedenii Aviatsionaya Tekhnika* (**1**) (1998) 49–53.
- [99] N. Kovalnogov, V. Kovalnogov, Characteristics of numerical integration and conditions of solution stability in the system of differential equations of boundary layer, subjected to the intense influence, *Izvestiya Vysshikh Uchebnykh Zavedenii Aviatsionaya Tekhnika* (**1**) (1996) 58–61.
- [100] S. Kottwitz, *LaTeX Cookbook*, Packt, Birmingham, 2015, pp. 231–236.